UNIVERSITY OF SOUTHAMPTON

FACULTY OF ENGINEERING AND APPLIED SCIENCE
DEPARTMENT OF ELECTRONICS AND COMPUTER SCIENCE

Signal Extraction Techniques For Self-Powered Micro-Systems

By

Edward Paul James

A thesis submitted for the degree of
Master of Philosophy

September 2003

UNIVERSITY OF SOUTHAMPTON

ABSTRACT

FACULTY OF ENGINEERING AND APPLIED SCIENCE
DEPARTMENT OF ELECTRONICS AND COMPUTER SCIENCE

Master of Philosophy

Signal Extraction Techniques For Self-Powered Micro-Systems

By Edward Paul James

Over recent years there has been a growing interest in the field of micro-systems and their applications across a wide range of areas, including sensor based micro-systems able to operate with full galvanic isolation. Two significant issues to consider when designing such remote sensor systems are the supply of power and the method of signal extraction.

In general terms this thesis develops the concept of a self-powered micro-system (SPMS), eliminating the need for a battery with a finite service life. Within the context of such a micro-system particular attention is given to signal processing and novel signal extraction techniques. Experimental work is explained and potential commercial applications for such novel remote sensor systems are proposed.

Acknowledgements

The author wishes to express his sincere gratitude to Professor Neil White and Dr Neil Ross for supervising this project. Their help, advice and guidance on a regular basis has been instrumental in ensuring that the project scope was kept within reasonable bounds.

The author also wishes to thank and acknowledge help from:

- Dr Michael Kraft, for agreeing to be the internal examiner for this thesis. His comments at an early stage of writing have helped greatly with the development of the thesis structure.

- Professor Andrew Brown, for providing the opportunity to study within his research group.

- The Engineering and Physical Sciences Research Council (EPSRC), for their financial support under grant number GR/M35086.

- The University of Southampton, for the provision of facilities.

Table Of Contents

List Of Figures

List Of Tables

List Of Symbols And Terms

a	Radius of the reader coil
b	Radius of the SPMS coil
B	Magnetic field *(as a vector)*
B_o	Strength of the arrival signal
f	Frequency of the arrival signal
I	Current
M	Mutual inductance between the two coils
N	Number of turns
r	Distance between the two coils
S	Surface area of the coil *(as a vector)*
V	Induced voltage
Q	Quality factor of the circuit
μ_o	Permeability of free space, $4\pi \times 10^{-7}$ (Henrys/metre)
Ψ	Magnetic flux through each turn
α	Angle of arrival of the signal
$\cdot$	Inner product of vectors *(i.e. cosine angle between two vectors)*

Glossary

A/D	Analogue to Digital
BW	Bandwidth
BPSK	Binary Phase Shift Keying
CCR	Corner-cube Retroreflector
CDMA	Code Division Multiple Access
CMOS	Complementary Metal Oxide Semiconductor
DD	Direct Detect
DS	Direct Sequence
Diversity	Use of multiple modalities
FDMA	Frequency Division Multiple Access
FEC	Forward Error Correction
FM	Frequency Modulation
ID	Identification
IM	Intensity Modulated
IR	Infra-red
MEMS	Micro Electro Mechanical Systems
ORNL	Oak Ridge National Laboratory
PEP	Peak Envelope Power
PEV	Peak Envelope Voltage
PWM	Pulse Width Modulation
PZT	Lead Zirconate Titanate
RF-ID	Radio Frequency Identification
SPMS	Self-Powered Micro-System
SS	Spread Spectrum
TDMA	Time Division Multiple Access
UWB	Ultra-Wide Band
QPSK	Quadrature Phase Shift Keying

Publications Resulting From This Work

This work has contributed towards numerous recent publications. It is predicted that more papers will result in the near future. The publications to date are listed below:

1. M El-hami, P Glynne-Jones, **EP James**, S Beeby, NM White, AD Brown, JN Ross and M Hill. *A new approach towards the design of a vibration-based microelectromechanical generator.* The 14th European Conference on Solid-State Transducers (27nd to 30th August 2000, Copenhagen, Denmark).

2. M El-hami, P Glynne-Jones, **EP James**, S Beeby and NM White. *Design analysis of a self-powered micro-renewable power supply.* International Conference on Electrical Machines (ICEM 2000), 27th to 30th August 2000, Espoo, Finland. ISBN: 951-22-5097-7, Vol.3, pp.1466-1470.

3. P Glynne-Jones, M El-hami, SP Beeby, **EP James**, AD Brown, M Hill and NM White. *A Vibration-Powered Generator for Wireless Micro-systems.* Published in the form of conference proceedings for the International Symposium on Smart Structures and Micro-systems (IS3M 2000), 19th to 21st October 2000, Hong Kong.

4. **EP James**, P Glynne-Jones, M El-hami, SP Beeby, JN Ross and NM White. *Planar Signal Extraction Techniques for a Self-Powered Micro-System.* Publication in the form of conference proceedings for the 6th annual conference on Sensors & Transducers (MTEC 2001), 14th to 15th February 2001, NEC, Birmingham, UK.

5. M El-hami, P Glynne-Jones, NM White, SP Beeby, **EP James**, AD Brown and JN Ross. *Design and fabrication of a new vibration-based electromechanical power generator.* Accepted for publication in the Journal of Sensors and Actuators on 11/12/00.

6. **EP James**, P Glynne-Jones, M El-Hami, JN Ross and NM White. *A planar interface for wireless micro-systems.* Accepted for publication in the form of

conference proceedings for "PREP 2001", 9th to 11th April 2001, Keele University, UK.

7. P Glynne-Jones, SP Beeby, **EP James** and NM White. *The Modelling of a Piezoelectric Vibration Powered Generator for Micro-systems.* Accepted for publication in the form of conference proceedings for the 11th International Conference on Solid-State Sensors and Actuators, 10th to 14th June 2001, Munich, Germany.

8. **EP James**, P Glynne-Jones, M El-hami, SP Beeby, JN Ross and NM White. A publication based on: *Planar Signal Extraction Techniques for a Self-Powered Micro-System.* A publication at the editors request for "Measurement and Control Magazine", an Institute of Measurement and Control publication.
Vol.34, Issue.2, March 2001, ISSN:0020-2940, pp.37-39.

9. **EP James**, P Glynne-Jones, M El-hami, SP Beeby, JN Ross and NM White. A publication based on: *Planar Signal Extraction Techniques for a Self-Powered Micro-System.* Published as part of a review for "Sensor Review Journal". ISSN 0260-2288, pp.190.

10. **EP James**, MJ Tudor, SP Beeby, NR Harris, P Glynne-Jones, JN Ross and NM White. *A Wireless Self-Powered Micro-System for Condition Monitoring.* Accepted for publication in the form of conference proceedings for the 12th International Conference on Solid-State Sensors and Actuators (15th to 18th September 2002, Prague, Czech Republic).

11. **EP James**, MJ Tudor, SP Beeby, NR Harris, P Glynne-Jones, JN Ross and NM White. *An investigation of self-powered systems for condition monitoring applications.* Submitted for publication in the Journal of Sensors and Actuators.

Chapter 1

1. Introduction

1.1 Overall Project Background And Scope

Applications exist for sensors without physical galvanic connection to their surrounding environment. Examples include self-powered micro-systems (SPMS) located on roads, bridges, fields, in the home, machinery and maybe even inside the human body. At present, communication with such sensors is often powered using a lithium battery[1]. Such batteries have a finite operational life, they can often be larger than the sensor and recent advances in integrated circuit technology of the type described by Moore's law have not been matched by similar advances in battery technology[2]. Batteries can therefore be seen as a significant obstacle when producing small micro-systems, based for example on MEMS technology.

A SPMS that does not require a battery, thus enjoying a greatly increased operational life would suit applications where the sensor is embedded or where a battery can not be easily replaced. Such systems that make use of ambient energy (that is the energy available in the SPMS surroundings, but is not stored explicitly) have a potentially longer operational life compared to battery based systems. The source of such ambient energy will inevitably depend on the given application. The most familiar ambient energy source is solar power from ambient light. Other possible sources of ambient energy are the flow of liquids or gases, energy produced by the human body[3], thermal energy[4] and the action of gravitational fields[5].

As well as natural (ambient) sources, power can also be supplied by an external source. Electromagnetic fields used in RF powered ID tags[6], inductively powered smart cards[7] and non-invasive pacemaker battery recharging[8] are just a few good examples of such an approach. All of these examples aim to increase the amount of energy that is available per unit volume in the system/sensors immediate surroundings.

In theory it should be possible for a self-powered micro-system to utilize ambient energy from within its surroundings to achieve reliable operation. It should also be possible for certain methods of communication to provide a source of power for the sensor, thus forming a possible hybrid link between power generation and communication with the sensors external environment.

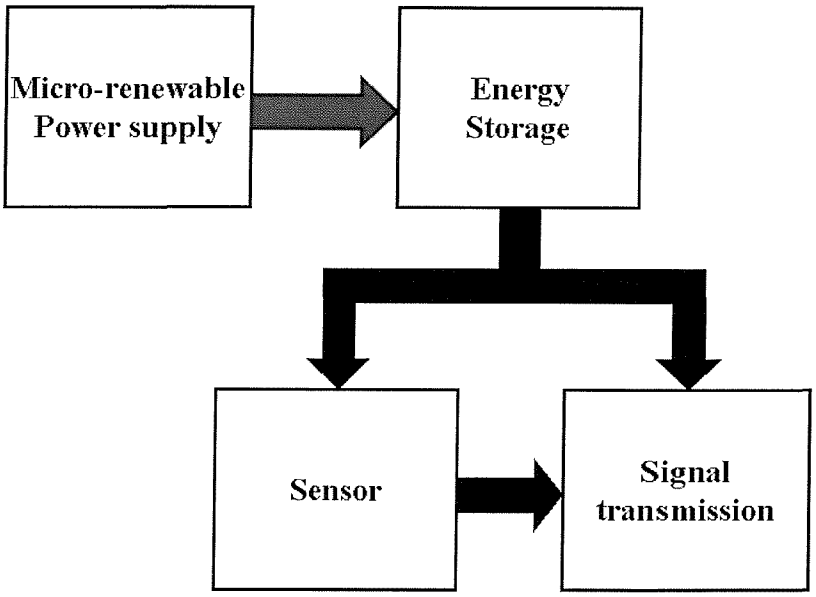

Figure 1: *Block diagram of a SPMS*

1.1.1 Advantages And Disadvantages Of Self-Powered Sensors

Table 1 shows some of the advantages and disadvantages of a self-powered sensor in relation to existing battery powered and hard wired sensors.

Sensor configuration	Advantages	Disadvantages
Hard wired	The sensor itself can be very small. High speed, reliable communications	The sensor can not be fully isolated. Not good for distributed sensors
Battery powered	No ambient energy is required	Limited life Larger size
Self-powered	A battery is not essential. Longer operational life	Reliable (ambient) energy source is required

Table 1: *Advantages and disadvantages of different sensor configurations*

1.1.2 Applications For Self-Powered Sensors.

Table 2 shows some example applications for Self-Powered sensors.

General application area for a SPMS	Specific examples
Roads	Gas (pressure) sensors embedded in pipes located under roads. This makes use of the implied intrinsic safety advantages
Bridges	Non invasive (i.e. pre-embedded) structural fatigue sensors
Fields	Periodic long term pollution monitoring
In the home	Small (i.e. no battery) wireless baby monitors, using vital life sign sensors
Machinery	Embedded oil pressure or mechanical fatigue sensors (e.g. in aeronautical structures)
Human body	Small distributed pressure sensors on artificial limbs

Table 2: *Applications for a SPMS with sensor input(s)*

Over the years there has been a growing interest in the field of miniature sensors and their wide range of applications such as medical implants, embedded sensors in buildings etc.. One specific area that has received little attention is how to supply the required electrical power to such sensors. Conventional power supplies external to such sensors is one way. However, many applications do require such sensors to be completely embedded in the structure with no physical connection to the outside world. Supplying power to such systems is difficult and as a result they need to have their own power supply unit making them self-powered micro-systems. Noise reductions, elimination of cross talk between power lines and signal lines, reduction of power delivery control systems complexity are just some of the potential advantages associated with truly integrated and self-powered micro-systems[9].

1.2 General Project Aim

To progress towards the creation of a self-powered micro-system with commercial potential.

1.3 Specific Project Objectives

Listed here are the main project objectives following on from the nine month report:

- Investigate into using mechanical systems able to convert ambient energy into useable energy for a SPMS.
  Model such mechanical systems.
  Develop different prototype designs. Optimise the design for maximum power, given reasonable size constraints.

- Evaluate the different feasible methods of signal extraction.

- Investigate voltage conversion/regulation circuits able to convert the output from a mechanical generator into a useable power source for a SPMS.
  Model the conversion circuits.
  Develop a prototype circuit(s).

- Develop a prototype micro-system.
  Integrate the power source/generator, the sensor, the processing circuit and other glue circuits to create a working demonstration system.

- Investigate using planar coils to transfer energy to a sensor system.
  Model planar coils able to transfer energy to a sensor system.
  Develop a number of different prototype designs. Optimise the coils, in terms of size, power, application, material, frequency etc.

- Investigate the possibility of using planar coils to extract data from a SPMS
  Model planar coils able to extract data from a SPMS.

Develop a number of different prototype designs. Optimise the planar coils, in terms of size, power, application, material, frequency etc.

- Compare and evaluate a range of micro-systems that use different methods of communication. Identify the key advantages and disadvantages of each approach.

1.4 Thesis Structure

Chapter 1: Introduction – This chapter provides an overview of the project and sets out the overall aims and objectives.

Chapter 2: Review of Self-Powered Micro-systems – This chapter looks at existing research relating to micro-systems and relevant standards.

Chapter 3: Development of a Vibration Based Power Generator – This chapter details the design, modelling, development and testing of a vibration based power generator for use within a self-powered micro-system. Key design parameters are identified and figures for available output power are given.

Chapter 4: Development of a LCD Based Micro-System Demonstrator – This chapter details the development of the first LCD based micro-system. The micro-system developed has an accelerometer input and the limits of operation have been determined. A shaker rig has been used to excite the micro-system and continuous operation has been achieved.

Chapter 5: Development of an Infrared Based Demonstrator – This chapter details the development of an infra-red based micro-system that is able to continuously operate over many centimetres. A new approach towards power conversion is proposed and the overall size and weight of the micro-system has been significantly reduced when compared with the LCD demonstrator described in the previous chapter.

Chapter 6: Development of a Planar Coil Micro-System Demonstrator – This chapter details the development of a micro-system that is able to communicate through a planar coil. Such a micro-system has the potential to be fully enclosed. Key design formula are identified and results specifically relating to the planar coil operation are described.

Chapter 7: Development of a Radio Micro-System Demonstrator – This chapter details the development of a micro-system that is able to communicate via a radio link. This method of communication arguably has most commercial applications. This is because a direct line of sight is not required for operation, as is the case for open optic communication. In addition, the distance between the SPMS and its receiver circuit is not limited to the order of centimetres, as is the case with the planar coil demonstrator. This chapter explores different aerial designs and the limits of operation for the power available.

Chapter 8: Conclusions – This chapter concludes the results of chapters 3 to 6. A comparison between the different micro-systems that have been developed has also been made.

Chapter 9: Future Work – This chapter highlights areas of future work that follow on from this thesis. Such work has the potential to push the current state of the art even further towards the development of a self-powered micro systems with commercial potential for a number of practical applications.

References – Full list of References.

Chapter 2

2. Review of Self-Powered Micro-systems

2.1 Overview

Because the micro-system can be divided up into self-contained blocks, it makes sense to review existing publications for each block in turn. An additional review of the system as a whole and relevant technology has also been provided. The following list details some of the desirable functionality for a complete system. It is well worth having these points in mind when reading this chapter of the thesis.

- An operational life that is significantly longer than existing battery based systems
- Communicate over adequate distances (something greater than one centimeter) reliably and securely, as required by the given application
- Avoid problems associated with EMI
- Provide compatibility with multiple standard products, as required
- Be suitably small (i.e. smaller or of similar size to existing battery based technology)
- Be self-powered, self-configuring, maybe even self-calibrating
- Be potentially cost effective to mass produce

2.2 Power Generation And Storage

2.2.1 Power Generation

The conventional solution to supply power is to use a battery, often containing lithium[1]. However, batteries only contain a finite amount of energy, have a limited life, can contain hazardous chemicals, can be quite bulky and often fail at inconvenient times. A better solution could be to develop a micro-generator able to convert energy from an existing ambient energy source into electrical energy.

Some possible ambient energy sources, which can be converted into electrical energy, include light energy, thermal energy, volume flow energy and mechanical energy[9].

Power in a self-powered micro-system will be in short supply, therefore the main objective is to ensure that power is efficiently used during the transmission of each sensor reading, hence a low data rate should be used, thus reducing the mean power consumption.

Linked into the idea of power generation using ambient energy is the need to store energy, thus forming a micro-system able to cope with fluctuations in both available energy and micro-system power demands.

Ideally an energy storage mechanism that can exhibit high power and energy densities with the smallest size possible is required. The following are possible solutions[9]:

- Electrochemical capacitors or super capacitors
- Rechargeable Lithium batteries
- Miniature flywheels
- Fuel cells
- Gas turbines
- Hybrid Solutions

2.2.2 The Use Of Super-Capacitors

The super-capacitor is a possible alternative to the true battery. Super capacitors make use of charge storage within a nanoporous electrode or on an electrode of extremely high surface area. Super-capacitors with capacitances in excess of $5x10^4$ F kg^{-1} have been available for several years and are used for energy storage applications in micro-power applications such as memory backup[10].

2.2.3 Vibrations

Low power design trends raise the possibility of using ambient energy (energy that is in the environment of the system and is not stored explicitly) to power future digital systems.

For an electromagnetic transducer calculations show that power in the order of 400μW can be generated[11]. It can be seen from figure 2 (as published in 1998) that just 100μW is enough power for sensors with low to medium throughput DSP to operate.

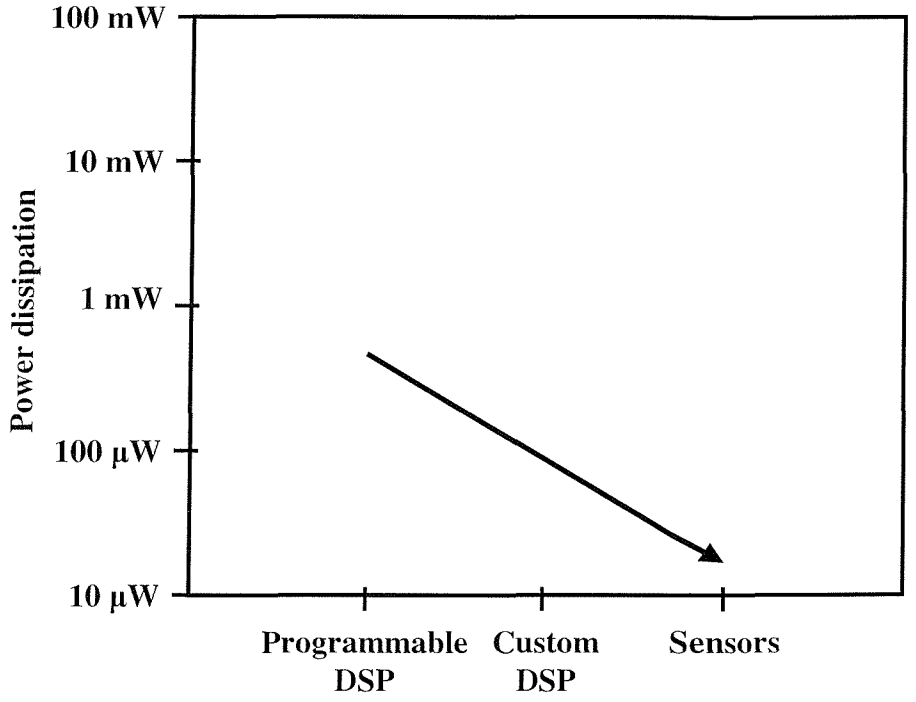

Figure 2: *Trends in power consumption for low to medium throughput DSP*[11]

One approach to generate electrical energy via transduction of mechanical vibrations is well demonstrated by Amirtharajah et al[11].

El-hami[12] et al also proposes a similar generator with power predictions of 0.2mW within a volume of less than 20mm^3 at a vibration frequency of 745Hz. Williams[13] predicts power generation of 1μW at 70Hz and 0.1mW at 330Hz for a device of around 5mm x 5mm x 1mm and a deflection of 50μm.

2.2.4 Using A Battery

Each application class has its own special requirements for batteries, based on electrical, mechanical, physical (i.e. weight and size) and environmental considerations as well as cost and accessibility for replacement. Battery life can be

seen as a function of how efficient the design is with respect to information conveyed per milliwatt hour of energy consumed, not how much power is used.

Since they were invented about 200 years ago, batteries have been developed and they are now common place in small electronic devices. New lithium ion polymer batteries not only solve the problems that have previously limited the acceptability of lithium in mass-market products but due to their size, weight and power density they are also a feasible solution as a means of micro-system power. Lithium is an ideal material for battery anodes because of its high intrinsic negative potential. Batteries based on lithium chemistries have the highest specific energy and energy density of all types.

2.2.5 Key Advantages Of Using Lithium Batteries

- They are about 30 percent smaller than a nickel cadmium battery with the equivalent power
- They are about 34 percent lighter than a nickel cadmium battery with the equivalent power
- Their solid state construction means they can be ruptured, torn, pierced and cut without exploding
- They don't contain toxic materials such as mercury or cadmium
- They have no significant memory effect
- Lithium is the lightest nongaseous metal and it is very reactive, it has a high energy density[11]
- Lithium batteries have low power-leakage rates compared to nicads
- The voltage per cell can be up to 4.2V instead of nicads 1.2V

2.2.6 Key Disadvantages Of Using Lithium Batteries

- They require a constant temperature, else hot spots within the battery can occur. For potentially low current applications like micro-systems this is not so pronounced.
- Recharge cycle times for a typical (NiCd) battery are say 500 to 1000 cycles, but lithium ion batteries tend to bow out well before such a typical battery.

	Operating Voltage (V)	Weight Energy Density (Wh/kg)	Remark
Lead Acid	1.9	30	Car battery, heavy & low density
Ni-Cd	1.2	40 ~ 60	Environment pollution, memory effect
Ni-MH	1.2	60 ~ 80	No memory effect but lower density than lithium
Li-ion Circular	3.6	90 ~100	No memory effect, thick diameter, explosive
Li-ion Prismatic	3.6	100 ~ 110	No memory effect, relatively thin, explosive
Li-ion Polymer	3.7	130 ~ 150	Thin, lighter, less explosive

Table 3: *Comparison of different battery technology*[14]

2.3 Signal Processing And Extraction

2.3.1 Communication With The Micro-system

Free-path optical or (planar) magnetic induction are possible techniques for communication provided the required range for communication is short (say less than 1m). Slightly longer range might be possible using radio and significantly greater range should be possible if the use of an optical fibre is acceptable[15], as has been demonstrated before[16,36].

A free-path optical communications link will generally have a much larger loss than one linked using an optical fibre, as much less of the transmitted signal will reach the

detector. However, provided the transmitted light can be collimated and directed to the receiver free-path optical communications may be viable over a short distance[15].

For some applications magnetic coupling using resonant inductive (planar) circuits is one technique, which may be expected to be viable when the required range is short. The size of the inductor will probably need to be small and this together with the dipole field of the inductor will severely restrict the range over which communication is possible. Magnetic coupling has the distinct advantage that it will not be highly directional, although correct orientation of the receiver coil will be required[15].

Radio telemetry may provide a solution where somewhat greater range is required. Again size is a problem as an efficient and preferably directional aerial would be required[15].

2.3.2 Analogue-To-Digital Conversion

The realization of signal sampling and quantization at high sample rates with low power dissipation is an important goal in many applications.

Analogue to digital converters can be very power hungry devices, hence the most energy efficient solution to encode the analogue signal from the sensor may be simply to use pulse position modulation[16].

Analogue-to-digital conversion techniques can be categorized in many ways. One convenient means of comparing techniques is to examine the number of "analogue clock cycles" required to produce one effective output sample of the signal being quantized[17]. Here an analogue clock cycle usually involves analogue operations such as comparison, D/A converter settling, operational amplifier settling, and so forth. The actual settling time required is of course both technology dependent and implementation dependent, but the number of cycles required for an effective conversion is a convenient means of comparison[17].

2.3.3 Trigger Circuits

Triggers are required to enable communication if the communication method is not continuous. The advantage of not using continuous communication is the availability of an increased power source during communication periods. The disadvantage is a reduction in the amount of information received from the sensor and the need to include (and power) a trigger circuit. There are very few publications in this important area.

For certain applications it makes sense to use embedded intelligence. This approach offers the most significant opportunity for energy management. The amount of data being transmitted directly affects battery life. For example, a sensor that transmits the entire spectrum from an accelerometer must sustain a higher data rate than one that can intelligently decide if the spectrum is normal and, therefore, may not need to transmit.

The more energy used to transmit a bit, the more likely it is that the bit will be received. Spreading the bit in spectral, temporal, spatial, or polarization domains (increasing diversity) makes it less likely that interference will corrupt the transmission. This is a trade off with throughput, though, because the more energy you put in each bit, the more energy needed for the total transmission. Embedded intelligence is key because it ensures that raw data is not transmitted needlessly.

2.3.4 Continuous Analogue/Digital Communication

Using continuous communication methods eliminates the need for a trigger, however there is an increased chance of loosing the communication link or receiving noisy data during periods of low power generation.

Continuous digital communication can be designed to use reduced power, because continuous communication does not always infer that continuous transmission is required. Communication protocols (like PWM) can help to significantly reduce the amount of average power required by the communication circuit.

2.3.5 Response To An External Stimulus

There is no point in transmitting a signal, if it is not required hence it makes sense to use an external trigger for communication, thus releasing information when it is required. The external trigger could take a number of forms and could even be a different communication technology to the primary transmitter (or actuator).

2.3.6 Transmission Based On Available Power

All practical communication methods will need to remain within the tight power limitations, however it may also make sense to use all of the available power, thus utilising more of the systems resources. This may mean communicating when there is enough power or (for some applications) communicating when there is a period of no/low power generation.

2.3.7 The Problem Of Using Standby Triggers

Any trigger circuit used would need to be powered constantly. This will cause a reduction in the available power for the communication circuitry. If the power source is not constant (as expected), then storage & regulation will be required, thus ensuring the trigger circuit remains active.

Powering the communication circuit using a trigger will create issues relating to circuit stability, as oscillators (and other glue logic) in the communication circuit will take time to become stable. This reduces the amount of useable time for communication and increases the amount of noise/error at the start of any transmission.

The transmission will only last for a finite length of time before the stored power is (almost) all exhausted. At this point the communication circuit will once again become unstable before communication stops.

The use of a trigger may define the period between transmissions, however the length of each transmission will be unknown (dependent on the amount of stored power). It

may be possible to use a second trigger to terminate transmission, however a better approach may be to just discard certain parts of any transmission.

2.4 Existing Micro-system Technology

2.4.1 RF-ID Tag Technology

In the 1960's development of a technology called *backscatter modulation* by the Lawrence Livermore Laboratories in the USA allowed for this communication to be implemented very simply and at low cost while keeping the required *frequency agile* characteristics of the transponder[18].

In 1998 Trolley Scan™ developed the Trolleyponder protocol, another protocol that could allow many (≈1000) transponders to be read at the same time with no tuned circuitry. It is practical today for transponders to be made in a single integrated circuit for a few US cents[18].

A compact tag form factor demands a small tag antenna, that in turn demands either external components or a high-frequency RF carrier for effective tag power delivery[19].

The front end is responsible for power recovery, demodulation of the incoming RF signal, and the backscatter transmission of return data. The remaining sections handle power management, biasing, data recovery, operating protocols, and user-available data storage[19].

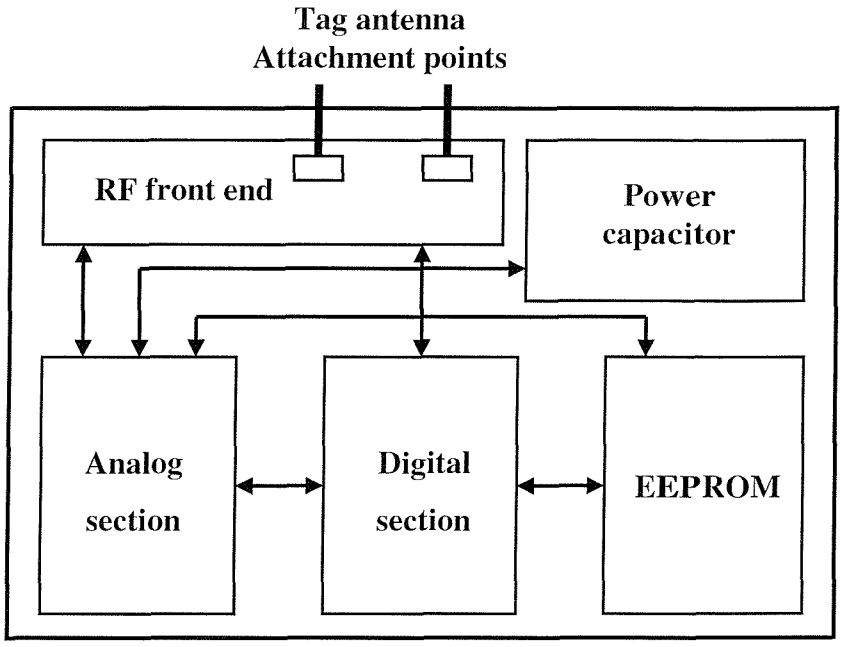

Figure 3: *Block diagram of an RF-ID tag*[19]

2.4.2 "Smart Dust"

SmartDust, a concept recently proposed by Kris Pister[20], are millimetre scale sensing and communication platforms composing a distributed sensor network that can monitor environmental conditions in both military and commercial applications[20].

The SmartDust power supply can be solar cells, button cell battery, or even a thin film battery. Uplinks of data are accomplished with an optical modulator.

There are several encoding methods available for intensity modulated/direct detect (IM/DD) channels like free space infrared.

Since the SmartDust data rate is 1 kbps or less, circuits can be run at very low speeds, and thus at very low voltages. This is the primary power reduction method.

Energy is minimal for low supply voltages and input signal rise/fall times.
It should be noted that (sub threshold operation is possible) even at such low supply voltages as 0.4V gates are still operational.

2.4.3 ORNL Bug Technology

Oak Ridge National Laboratory's first miniature wireless device, an IR beacon that was designed to track killer bees over a range of about 2km[21] has no internal energy storage in the form of a battery. The device can be made at low cost and have a long shelf life. The energy is provided to the system by means of a solar cell, and energy is stored on a capacitor.

2.4.4 Seiko Wrist Watch Technology

Seiko have invented two interesting Micro-systems[5]. Both micro-systems are in the form of a watch, but they use different sources of ambient power. The first watch can harvest energy from the motion of the wearer (Seiko Kinetic), using a miniature mechanical generator. The second watch harvests it energy from body heat (Seiko Thermic), using the Seebeck effect. Stordeur[22] has also published similar work on a *Thermoelectric generators.*

2.5 Standards

There are numerous standards that may become relevant to self-powered micro-systems. There are two main areas to think about. Standards required for the sensor to be used in niche applications, for example in an intrinsically safe environment and standards relating to use of the electromagnetic spectrum for communication/energy transfer (for example the first over-the-air standard IEEE 802.11, as used by wireless Ethernet).

Standards tend to change, depending on geographical location (e.g. Europe Vs the United States of America), however it normally makes sense to try and meet the strictest standard, thus providing increased usability.

2.5.1 Standards For Intrinsically Safe Areas

The british standard for electronic equipment for use in a hazardous environment, BS 5501, requires that for equipment to be excluded from certification no voltage must exceed 1.2V, no current 0.1A, no stored energy 20μJ and no power 25mW[23].

Both voltage and stored-energy requirements are hard targets for a self-powered micro-system to meet[36].

2.5.2 Standards For Protocols And The Electromagnetic Spectrum

ISO/IEC has announced a new standard designated ISO/IEC 15693-2 which specifies how data is passed between RF-ID tags and readers. It is specific to the 13.56MHz frequency, and covers RF-ID tags commonly referred to as "smart labels". RF-ID technology operating in this band uses magnetic propagation offering read/write performance with anti-collision features and with read ranges typically up to 50cm and write ranges of 25cm. Actual performance is dependant on the reader coil sizes[24].

Generally each country in the world manages its own radio spectrum and treats the radio spectrum as a national resource. These plans have evolved over time depending on the needs of the users and industry in those particular countries, resulting in virtually no uniformity of spectrum with application over the worlds regions[25], however detailed information on current frequency ranges and licensing regulations is published[26].

In order to bring a measure of uniformity, the world has recently been divided into three regulatory areas. Uniformity will however only be achieved towards the year 2010 as it requires each country to implement the plans for that region[25]. The regions are:

- Europe and Africa (region 1).
- North and South America (region 2).
- Far East and Australasia (region 3).

Each of these bands has specific requirements that have to be met, for example power, frequency stability, interference and priority.

The basic frequency bands in which RF-ID type activities occur in some of the regions around the world are:-

- Less than 125kHz

- 1.95 MHz/ 3.25MHz/ 4.75MHz and 8.2MHz
- 13.56 MHz
- Approx 27 MHz
- 430-468 MHz
- 856 MHz
- 869 MHz
- 902-928 MHz
- 2350 - 2450 MHz
- 5400 - 5900 MHz
- 24.125 GHz

Standards are constantly being updated for technical, political, commercial and other reasons. New standards are also created from time to time, however these are often based on existing technology. One such example (incorporated in the IEEE 802 standard as IEEE 802.15) is the new wireless Bluetooth standard. Although many detractors argue that it is not suitable for industrial measurement. Bluetooth operates in the 2.4GHz band with a limited range. It is designed and marketed for home and office automation environments.

2.6 Technology Feasibility

2.6.1 Overview

The main contenders for "cabless" transmissions are optical, infra-red and radio-based systems[27]. Significant advances in reducing the requirement for numerous galvanic connectors came about with the introduction of local area networks[27]. For many applications wires are not acceptable, for example where isolation is necessary for noise reduction or safety[28].

There are numerous techniques for isolated signal-coupling, including transformers, differential-capacitor and opto-isolators. Each method has its own advantages and disadvantages, for example transformer coupling has high inter-winding stray capacitance and a tendency to couple switching noise into the signal.

2.6.2 Powering The Micro-System

It is important to get a feel for the different potential sources of power, because this may help to provide an indication as to how much power could be available for use by the signal processing and communication circuits. Once there is sufficient power for the micro-system to be feasible, any additional power can be used to increase the micro-system communication range.

2.6.3 Solar Or Open Optics

Kuntz[29] proposes a smart sensor which is energized by daylight. Approximately 10mW of electrical power is obtained from a $0.1m^2$ solar panel in ambient room conditions (800 lux). $0.1m^2$ would be a very large area for a SPMS to utilise, however the implication is that an area sized just $0.01m^2$ would potentially produce 100μW. This is still a workable order of magnitude.

2.6.4 Fibre Optics

A number of authors, for example Ross et al[16] and Kuntz et al[29], have described optically powered sensors in detail. For good coupling, the diameter of the fibre must at least equal the size of the active area of the laser array (typically 100 – 200 μm in one dimension)[29]. Fibre optics may provide both communication and power transmission for a sensor or actuator unit[29]. Optical-fibre based sensors are useful where electromagnetic interference is rife or where there is a need to operate at an elevated electrical potential[36]. The efficiency with which optical power may be converted to electrical power is typically about 10%[36] (but can be about 30% for GaAs).

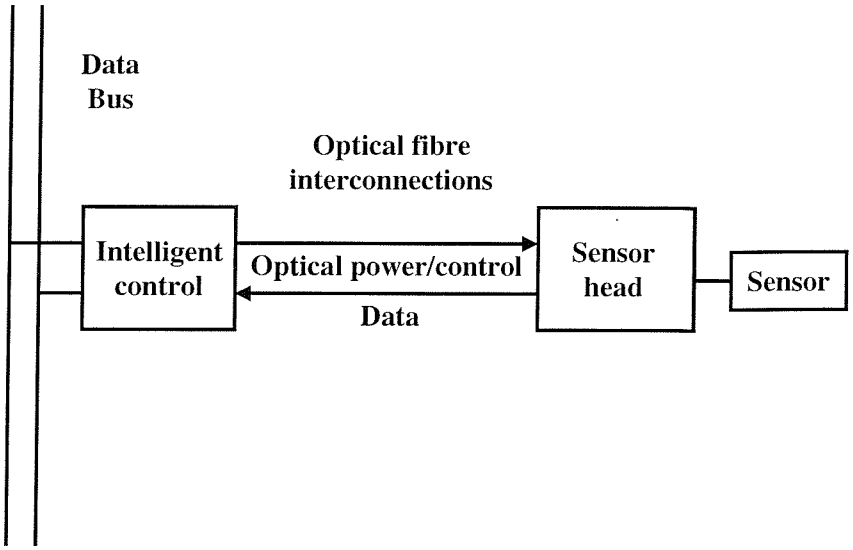

Figure 4: *An optically powered sensor system*[36]

2.6.5 Induction

Power induction has been about for a long time and is now being used in contact-less smart card applications. Smart cards equipped with a chip, instead of a magnetic ribbon, are becoming widely used due to the reliability at system level[7]. One of the reasons for this trend has been the development of planar coils. Such coils have a very low profile (in one plane) when compared to a more traditional 3D coil, but obviously planar coils are still 3D.

Planar inductors (and indeed larger scale true three dimensional coils) are starting to find real life applications and lots of work is currently being done on issues such as planar shape design and planar performance[30].

Matsuki has published information on a planar transformer (70 x 30 x 1mm^3). The trial design can supply a power of 6W[31]. The transformer consists of Co-based amorphous magnetic fibres with zero magnetostriction and conducting fibres. Features of the transformer include a thin planar shape, high flexibility and low waste heat because of use of amorphous (120μm) magnetic fibres[31].

2.6.6 Design For Low Power Consumption

Several architectural approaches facilitate low power operation. For applications requiring a processor-like controller, RISC architectures are suitable for low energy design, since they reduce the number of steps required to execute a task. Low energy RISC processors are often used in CMOS watch circuits and in embedded microprocessors[32].

Use of components that only require a unipolar supply[33] and a low operating voltage can help to reduce power demands.

Sensors built with silicon technology are available for thermodynamic applications such as temperature and pressure measurement. Temperature sensors can use properties of semiconductors such as dependence of p-n junction current on temperature. Pressure and acceleration can be measured with silicon strain gages, which rely on electron or hole mobility changes with mechanical stress. Some signal conditioning circuitry has been added to this class of sensors, and more integration should be possible[34].

VLSI CMOS technology is well suited for sensor signal processing applications because of its low power dissipation, high speed, and tight packing density. This allows complex circuits like sensor microprocessors to be built which can operate from batteries while running with megahertz clock rates[34].

Low-voltage, very-low-current integrated circuit techniques were originally developed more that 25 years ago for the watch, one of the first very large scale exploitations of CMOS technology. Modern watch circuits have a complexity ranging from a few thousands to several tens of thousands of transistors, combine microcontroller architectures with some high performance analogue circuits, and are routinely produced in tens of millions per year with a power consumption below 0.5μW at 1.5V[35].

In analogue circuits, the absolute limit comes from the need to maintain the energy of the signal much larger than the thermal energy, to achieve the required signal to noise

ratio S/N. This condition can be expressed as a minimum power per functional pole $P_{min} = 8fkTS/N$, where f is the signal-frequency bandwidth[35].

In digital systems, each elementary operation requires a certain number m of binary-gate transition cycles, each of which dissipates an amount of energy. The number m of transitions is only proportional to some power of the number of bits N_{bit}, and therefore power consumption is only weakly dependent on S/N (essentially logarithmically). Comparison with analogue is obtained by estimating the number of gate transactions required to compute each period of the signal, for example $m=50N_{bit}^2$. Immunity to thermal noise imposes an absolute minimum energy per transaction E_{trmin} estimated at 8kT, which provides the absolute minimum power limit[35].

2.7 Summary Of Attributes For Different Methods of Communication

Table 4 shows a summary of attributes for different communication methods. It can be seen from this table that there is no obvious method seen to be better than others in its field. There are advantages and disadvantages associated with each method.

Attributes	Communication technology				
	Ultrasound	**Radio frequency/far field**	**Planar Coil/near field**	**Fibre optics**	**Open optics**
Operational range	Tens of metres	Many metres	A few metres	No limit	Many metres
Causes electrical noise/RFI	Yes	Yes	Yes	No	No
Is affected by electrical noise/RFI	Yes	Yes	Yes	No	Yes
Secure	No	No	Yes with care	Yes	No
Robust connection	No	No	Yes most of the time	Yes	Yes most of the time
Cost	Low	Medium	Medium	Medium/high	Low
Implementation size	Centimetres	Centimetres	Many centimetres	Centimetres	Centimetres
Power requirements	Low	Medium	Medium	High	Very High
Data transfer rate	Medium	High	Medium/high	Very high	Very high

Table 4: *Summary of attributes for different communication methods*

2.7.1 Summary Of Wireless Sensor Attributes And Technology

Table 5 summarizes the desired attributes for wireless sensors and the technologies being used to provide those attributes.

	Technology									
Attributes	DSSS FHSS UWB	CDMA TDMA FDMA	Low-power designs	Mobile ad hoc networks	Power Harve-sting	Embeded Intellig-ence	Diver-sity	FEC	Open stand-ards	BPSK QPSK M-ary
Long Range	NA	NA	NA	Yes	NA	NA	Yes	Yes	NA	NA
Plug-and-Play	DSSS	CDMA	NA	NA	NA	NA	NA	NA	Yes	NA
Long Battery Life	FHSS	FDMA	Yes	NA	Yes	Yes	Yes	Yes	NA	M-ary
Low RFI risk	DSSS	NA	Yes	Yes	NA	Yes	Yes	NA	NA	NA
Self-locating	DSSS	CDMA	NA	NA	NA	Yes	Yes	NA	NA	NA
Secure	UWB	CDMA	Yes	NA	NA	Yes	Yes	NA	NA	NA
High throughput	UWB	NA	NA	NA	NA	Yes	Yes	Yes	NA	M-ary
Non line-of-sight	UWB	NA	NA	Yes	NA	NA	Yes	NA	NA	NA
Robust connections	DSSS	CDMA	NA	Yes	NA	NA	Yes	Yes	NA	BPSK
Low cost	FHSS	FDMA	Yes	NA	NA	NA	NA	NA	Yes	BPSK
Small size	FHSS	TDMA	Yes	NA	NA	NA	NA	NA	NA	BPSK

Table 5: *Summary of desired attributes Vs technologies for wireless sensors*[21]

A "Yes" implies that the technology offers an advantage in providing the functionality in the attributes column and "NA" is listed where no particular advantage exists for that technology in facilitating the attributes.

The relative weights of the attributes will be a function of the particular application. The critical question is always what trade off was made to get the property of interest. Here are a few examples:

- Battery life can be extended at the expense of update rate or response time.

- Range can be increased with increased transmitter power, but that could cause more interference or reduce the battery life.
- Throughput can be increased, but at the cost of battery life and interference.

Transmission using a variety of possible coding schemes could help to reduce the mean power required, even if the sensor signal was digitised[36].

2.7.2 Summary Of Published Information

It has become clear to the author that there has been a lot of information published on Analogue-to-digital converters, remote power generation, PZT properties & applications, optics as a power source and battery technologies.

There has not been much information published on (high level) hybrid design for self-powered sensors (e.g. combining power supply with signal extraction), trigger circuits for optimal usage of power, self-powered sensors and very low power voltage converter circuits.

There have only been a limited number of publications in the area of voltage conversion (μV to V). There are a few basic circuits published for stepping up voltages[37], however these circuits will not all work in the μV range.

The gaps in existing literature suggests that this project could become very rewarding, as there are several potentially novel areas that can be investigated further.

Chapter 3

3. Development of a Vibration Based Power Generator

3.1 Introduction

This chapter details the design of a vibration based magnet-coil power generator for use in the Self-Powered Micro-System, as described in the following chapters. Key design parameters have been identified and these have been used to develop a prototype generator that is able to operate at frequencies that are not unreasonable for real life applications such as condition monitoring. Testing of the prototype generator on a shaker rig is described and typical values for generated power are stated. This work has led to three publications, as stated at the start of this thesis.

3.1.1 The Vibration Based Generator

A schematic diagram of the electromechanical power generator, illustrating dimensioned and labeled drawings of beam/magnet assembly is shown in figures 5 and 6 below.

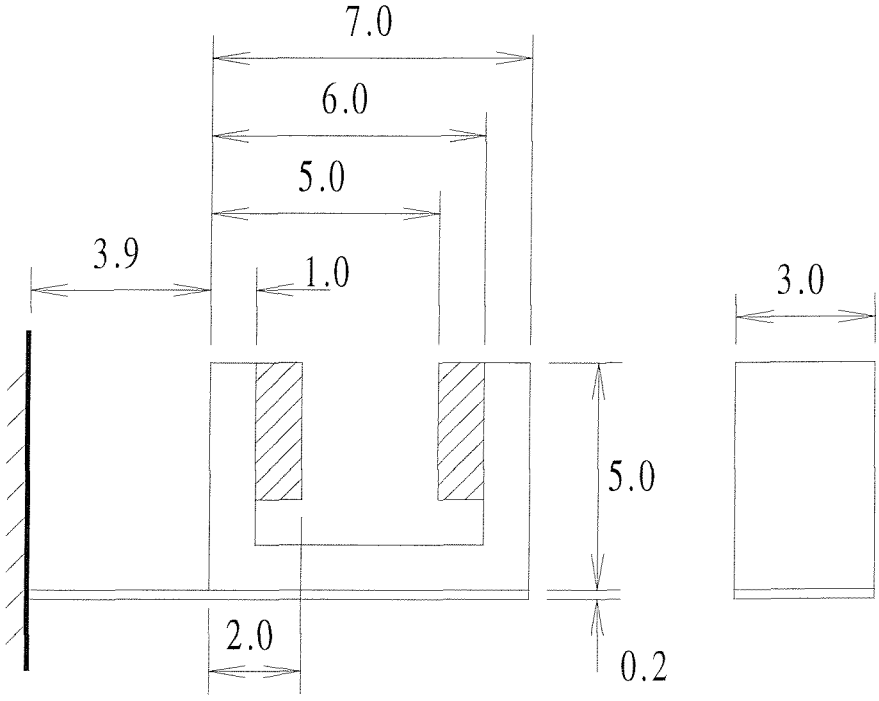

Figure 5: *Schematic of the electromechanical power generator*

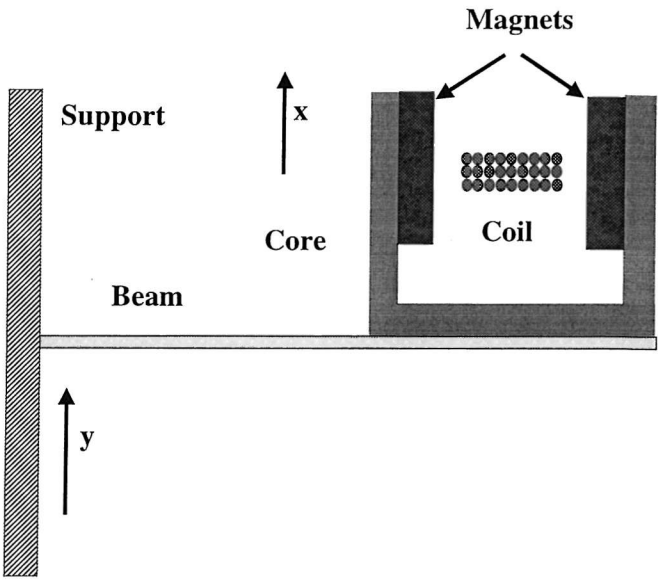

Figure 6: *Physical design of the electromechanical generator*[21]

The system consists of a cantilever beam supported by the housing. The mass on the beam consists of two magnets (one pole) mounted on a c-shaped core. Arranging the magnets in this way provides a uniform magnetic field in the air-gap. The core is designed to guide the magnetic flux with the minimum amount of flux leakage. The coil is made up of a number of single solid core enamelled copper wires. It is placed in the air-gap between the magnets at right angles to the direction of the movement of the mass.

The operating principle of the device is as follows; As the housing is vibrated, a mechanical input force feeds into a second order mechanical system, the mass moves relative to the housing and energy is stored in the mass-beam system. This relative displacement, which is sinusoidal in amplitude, causes the magnetic flux to cut the coil. This in turn induces a motional electromotive force on the coil due to Faraday's law. The magnitude of this voltage is proportional to the rate of change of the coil position. The electrical system involved is simply a first-order LR circuit with the inductance of the coil in series with the load resistance and the parasitic resistance of the coil.

3.1.2 Design Analysis

In order to determine and predict the practical performance of the device electromechanical and magnetic analyses have been undertaken.

Consider the system shown in figures 5 and 6 to consist of a point mass (m) mounted on the end of a beam providing a spring stiffness k. Variables x and y are the displacements of the effective mass and the vibration housing respectively. It is assumed that the mass of the housing is much greater than m and movement of the housing is unaffected by the movement of the generator. For a sinusoidal excitation $y = Y\sin\omega t$, where Y is the amplitude of vibration and ω the angular frequency of vibration, the following differential equation of motion is obtained[38].

$$m\ddot{z} + c\dot{z} + kz = m\omega^2 Y\sin\omega t \tag{3.1}$$

where z is the relative displacement of the mass with respect to the vibrating body, $z = (x - y)$, k is the beam stiffness and c is a damping coefficient. The solution to equation (3.1) is given by:

$$z = \frac{m\omega^2 Y}{k - m\omega^2 + j\omega c}\sin\omega t \tag{3.2}$$

The instantaneous electrical power, P_i, generated by the system is

$$P_i = c_e\dot{z}^2 \tag{3.3}$$

Where c_e is the portion of the damping attributable to electrical power generation.

Hence the magnitude of the generated power, $|P_i|$, is

$$|P_i| = c_e \left| \frac{mY\omega^3}{(k - m\omega^2) + j\omega c} \right|^2 \tag{3.4}$$

and the generated power may be written as:

$$P = \frac{m\varsigma_e Y^2 \left(\frac{\omega}{\omega_n}\right)^3 \omega^3}{\left[1 - \left(\frac{\omega}{\omega_n}\right)^2\right]^2 + \left[2\varsigma\left(\frac{\omega}{\omega_n}\right)\right]^2} \tag{3.5}$$

where $\omega_n = \sqrt{\frac{k}{m}}$ is the natural frequency of the system and $\varsigma_e = {}^{c_e}/_{2m\omega_n}$ is the electromagnetic transducer damping factor. The overall damping factor of the system, ς, includes losses due to friction, air resistance, etc., ς_f, and is given by:

$$\varsigma = \varsigma_e + \varsigma_f = \frac{c}{2m\omega_n} \tag{3.6}$$

The voltage, e, and current, i, generated within the system can be described by the following equations:

$$e = \phi\dot{z} - i(R_c + j\omega L_c) \tag{3.7}$$

$$F_e = \phi i \tag{3.8}$$

where F_e is the force generated by the electromechanical coupling, R_c and L_c are the resistance and inductance of the coil respectively and the transformation factor ϕ is:

$$\phi = NBl \tag{3.9}$$

Here, N is the number of turns, B is the average flux density in the air-gap and Nl is the effective length of coil.

If the current is driving a load of resistance R_L, the electrically generated force will be

$$F_e = \frac{\phi^2 \dot{z}}{R_L + R_c + j\omega L_c} \tag{3.10}$$

Hence the electrically generated damping, c_e, will be

$$c_e = \frac{\phi^2}{R_L + R_c + j\omega L_c} \tag{3.11}$$

and at frequencies where the inductive impedance is much lower than the resistive impedances, the electrically generated damping ratio will be:

$$\varsigma_e = \frac{\phi^2}{2m\omega_n (R_L + R_c)} \tag{3.12}$$

Operating the device at resonance, when $\omega \approx \omega_n$ (as we're considering relatively high Q systems), and substituting from equation (3.12) into equation (3.15) gives the total electrical power generated as:

$$P = \frac{\phi^2 Y^2 \omega_n^{\ 2}}{8\varsigma^2 (R_L + R_c)} \tag{3.13}$$

3.1.3 Determination Of Design Parameters

For determination of the design parameters, both analytical and numerical techniques have been employed. Analytical design programmes implemented in MatLab environments are specifically tailored to calculate the physical parameters, dimensions and other functional requirements of the device. A general-purpose electromagnetic field analysis CAD software package (VF-OPERA) that uses finite element methods has been used to model and solve the magnetic field distribution in a range of design variants of the device[39]. The design parameters are iteratively refined, ultimately resulting in the optimum design.

For convenience and ease of fabrication an arbitrary size (thickness and cross-section area) for the magnet and a relatively large air-gap of 3 mm has been chosen. The core thickness is determined by the need to carry the magnetic flux in the circuit without exceeding a nominal saturation flux density of 1.6 Tesla. The core and magnets are modeled in X-Y symmetry in OPERA-2d by drawing their exact geometry as a set of non-overlapping regions. Their B-H characteristics are defined by curve fitting and to calculate the flux density in the air-gap non-linear static solution of the system is performed. The natural frequency of the beam is calculated using Rayleigh's energy method, so as to allow for the distributed nature of the mass on the beam and for rotational inertia effects. In order to keep the natural frequency of the beam low, a thickness of 0.2 mm and a total length of 10mm were chosen. The effective mass of the magnetic core assembly is about 500mg the beam width 3mm and the natural frequency of the beam is calculated to be 327 Hz.

3.1.4 The Prototype

Hard permanent magnet (PM) materials such as samarium-cobalt and neodymium-iron-boron (NdFeB) materials have straight demagnetization curves throughout the second quadrant of their B-H loop. The latter is more popular in high performance applications and is much cheaper than samarium cobalt. For this application, neodymium-iron-boron 34KC1-grade material has been used. The remanence flux density (Br) and the recoil permeability (μ_{rec}) of the magnet employed are 1.2 Tesla and 1.04 respectively. The choice of material for the core once again is largely dependent on performance and, of course, the cost. In this application, mild steel with a nominal saturation flux density of 1.6 Tesla has been utilised. The coil has been made up of three layers each containing nine single turn solid enameled copper wires. Each wire has a diameter of 0.2mm. The cross-section of the coil has a nearly rectangular shape. There is a range of magnetic and non-magnetic materials that can be used for the beam. Electromagnetic field distribution analyses have shown that the average flux density in the air-gap is not affected by the choice for the beam material. Therefore, stainless steel is used for the beam. The core and the beam have been machined with a tolerance of ±0.07mm while the magnets have been manufactured with a tolerance of ±30μm. These were mounted together using a suitable adhesive material.

3.1.5 Test Arrangement

A Goodman V.50 Mk.1 (model 390) Vibration Generator (shaker) is used to supply mechanical vibrations to the device under test. A Ling PA50VA amplifier is used to drive the shaker. The amplifier is driven from the frequency source incorporated into a Hewlett Packard HP35660A Dynamic Signal Analyser. The device is mounted on the shaker using a specially designed clamp. An accelerometer (Bruel & Kjaer Type 4369) is mounted axially above the spindle on a short thread. The accelerometer provides data on the amplitude of vibrations applied to the device, which can not be determined solely from the electrical drive to the shaker, due to the non-linear response of the shaker. The accelerometer has a first resonance at 36kHz, which is well above frequencies of interest in the experiments conducted for this application. The clamp consists of an aluminum plate on an aluminum base, held in place by a pair of bolts through each plate. The end surfaces are machined with the plates in position to ensure that the end surfaces of the plates and the base lie in the same plane. The clamp is designed to act as a former for the voice-coils, holding them securely in relation to the beam. Figure 7 shows the block representation of the experimental setup.

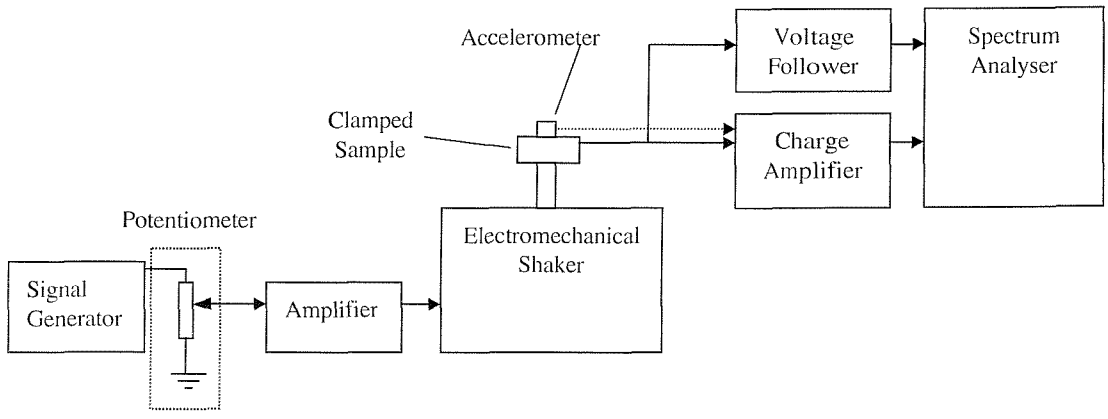

Figure 7: *Block representation of the experimental setup*[21]

3.1.6 Discussion Of Results

Modeling the design parameters discussed above, the theoretical load voltage and maximum useful output generated power from the device were first calculated for a range of amplitudes of vibration. Figure 8 illustrates the variation of load voltage with the amplitude of vibration.

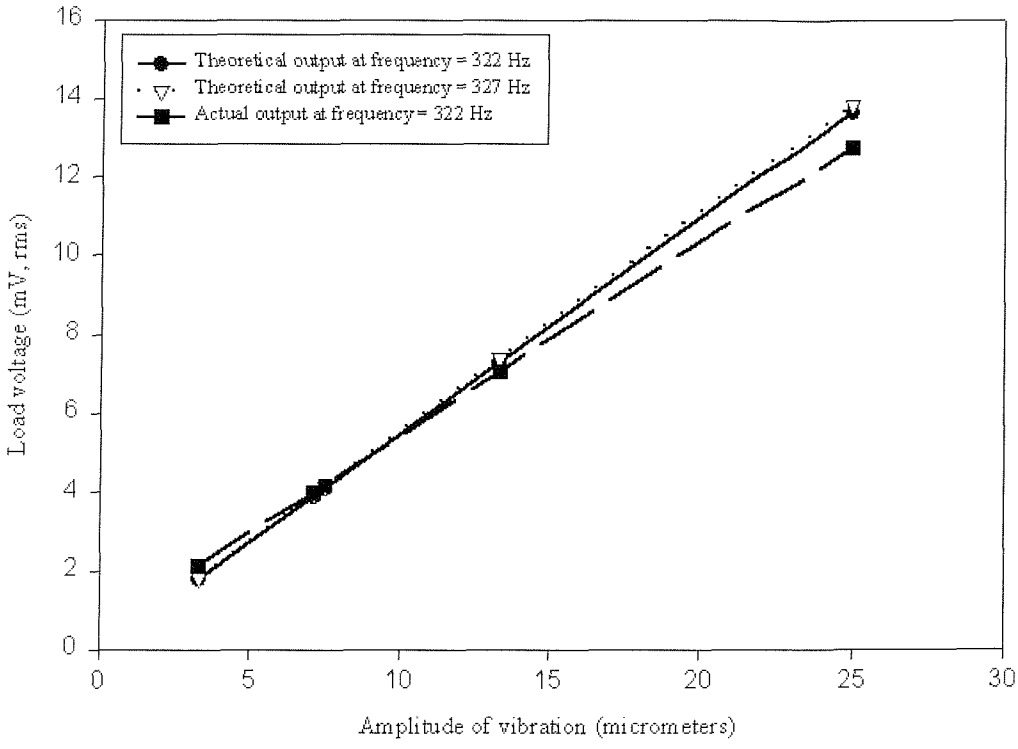

Figure 8: *Variation of load voltage with the amplitude of vibration.*

Following the fabrication of the prototype and its assembly, the actual resonant frequency of the system was found to be 322 Hz. The solid line in Figure 8 demonstrates the calculated variation of the load voltage with increasing amplitude of vibration corresponding to the actual measured resonant frequency of 322 Hz. The same figure also shows the corresponding curve obtained from experimental results which is shown in broken line. It is clearly evident that as the amplitude of vibration increases causing an increase in the maximum deflection, the difference between the measured and calculated results becomes greater. One of the factors causing this is, of course, the difference between the simulated and fabricated design parameters. Other factors include the non-linearity's associated with the system not considered in the modeling. Factors like the non-linearity of magnet movement with respect to the coil

as it is deflected through a larger distance and the non-linear variation of the magnetic field in the air-gap. The former non-linearity effect can cause a maximum reduction of 7% in the magnitude of flux density acting on the coil and the latter can lead to a maximum reduction of almost 9% in the magnitude of flux density in the air-gap. Another factor contributing to the differences between the measured and calculated figures is the unwanted damping factor, which is extremely difficult to predict accurately. However, based on experimental data an unwanted damping factor of 0.013 has been used in these experiments.

The results indicate that a maximum useful output power of 0.53 mW with amplitude of vibration of 25μm has been generated. This power corresponds to a maximum deflection of 0.94 mm at a resonant frequency of 322 Hz. It should be appreciated that the results do not represent the best-case estimate of the proposed scheme. The prototype fabricated has the potential to be optimised further to improve the performance. For example, it can easily accommodate a higher number of turns, which greatly increases the output voltage. With careful arrangement of the coil, making it shorter in length, losses are greatly reduced and the generated power increased. The air-gap can be further reduced and magnet thickness increased to improve the magnetic field in the system. The results generally show that the device is capable of generating a practical amount of power at relatively low frequencies. Such an amount of power can meet the requirement of a variety of systems such as low power very large-scale integrated (VLSI) circuits.

3.1.7 Conclusions

Generation of electrical power from mechanical vibration has been studied. An electromechanical power generator whose operating principle is based on the relative movement of a permanent magnet with respect to a coil has been designed and fabricated. The feasibility studies and experimental results have demonstrated the potential of such a device for self-powered systems. The prototype occupies a maximum space of 240mm^3 including the space required for the maximum deflection. Within this space, generation of useful electrical power of 0.53mw has been practically achieved. This power corresponds to 25μm amplitude of vibration at an excitation frequency of 322Hz. The results have clearly shown that generation of

practical amount of power within a small space is now possible and that the elimination of batteries for certain applications with modest frequencies looks feasible.

Chapter 4

4. Development of a LCD Based Micro-System Demonstrator

4.1 Introduction

This chapter details the design and development of the first stand alone self-powered micro-system (SPMS). The system power is provided by the magnet-coil generator excited by ambient vibrations described previously in chapter 1. The key components of the micro-system are:-

- A magnet-coil generator. This is mounted on a Goodman V.50 Mk.1 (model 390) Vibration Generator (or shaker) to simulate different real life environments.

- Conversion circuitry to handle stepping up the generator output voltage, rectification and regulation.

- An accelerometer with a digital output (Analog Devices^{TM} model ADXL202).

- A low power liquid crystal display (Lascar Electronics Ltd. model DPM 1S).

At this stage, the demonstrator has not been developed for a specific application. The use of an accelerometer is consistent with applications such as condition monitoring where the frequency of vibrations can provide information on the health of industrial machinery. An operating frequency of around 100Hz has been chosen because this is also consistent with such condition monitoring applications. For example, 100Hz vibration caused by a minor fault in a bearing cap within heavy machinery is described by Jackson[40]. The SPMS will function in such an application provided there is continuous environmental vibration of suitable amplitude and frequency.
For the initial SPMS a simple Liquid Crystal Display (LCD) has been used to relay information. This continuously displays the accelerometer output on the LCD for visual inspection as required.

The objective of this part of the thesis was develop an operational vibration based micro-system, and to optimise the design parameters in order to maximise the efficiency of each system block. Figure 9 shows a block diagram of the demonstrator system. Energy efficiency and functionality are the key design considerations of each component of the micro-system.

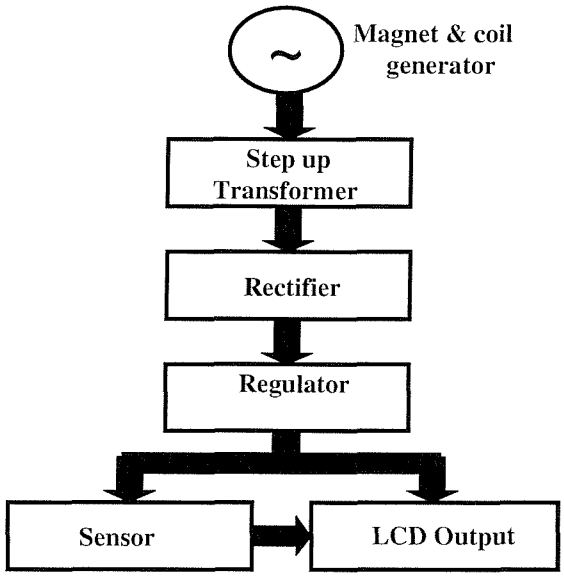

Figure 9: *Block diagram of the first SPMS to be developed*

4.2 Characterization of the Generator

The generator powering the SPMS is shown in figure 10 and has been documented by Glynne-Jones et al[2]. Neodymium Iron Boron magnets are mounted on a stainless steel beam (0.3mm thick, 13mm wide and 27.7mm long) that oscillates about a copper coil with a mechanical resonant frequency of around 100Hz. For a given application, the generator needs to be mounted on a vibrating structure and this has been simulated in the lab by using a shaker rig comprising of a Goodman V.50 Mk.1 (Model 390) Vibration Generator. This rig can produce vibrations in the range of 5Hz to 4kHz (this is limited by the current consumption of the coil and the rigs first unloaded structural resonance frequency of 5kHz). The vibration generator is controlled by a Hewlett Packard HP35660A Dynamic Signal Analyser driving a Cambridge Audio 65W integrated amplifier. A displacement of the magnet of 0.4mm at the generator

fundamental resonant frequency of 102Hz produces approximately $0.5V_{rms}$ and a constant power of 1.25mW.

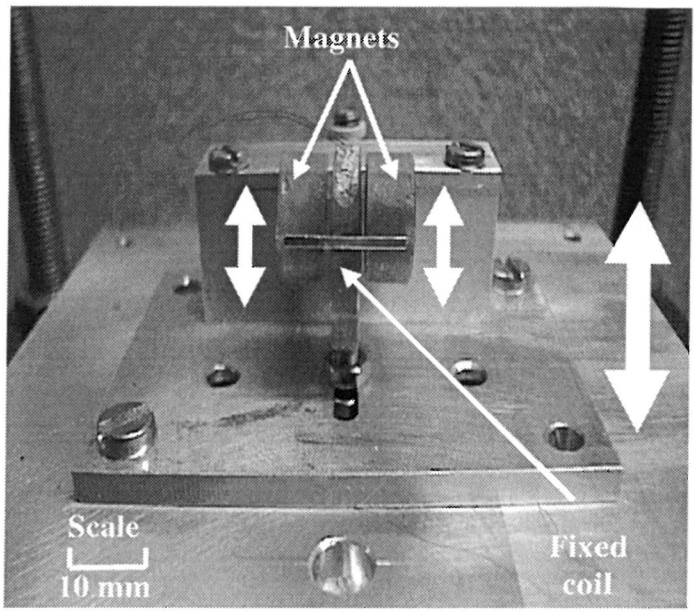

Figure 10: *A prototype vibration based power generator*

Figure 11 shows a spectral analysis of the micro power generator's output when driven by a shaker rig between frequencies of 0 and 800Hz. This was measured by driving the shaker rig with a random spectra of frequencies (from the Hewlett Packard HP35660A Dynamic Signal Analyser) and measuring the generator's output directly on the same analyser. Point A represents 50Hz mains noise, point B represents the fundamental resonant frequency of the power generator at 102Hz, points C and D represent other torsional and harmonic modes. The resonant frequency of the generator can be easily tuned to a given application by changing the length of the steel beam holding the magnets. Since the power increases with frequency ($P\alpha f^3$), harmonic frequencies also have the potential for generating useful amounts of power.

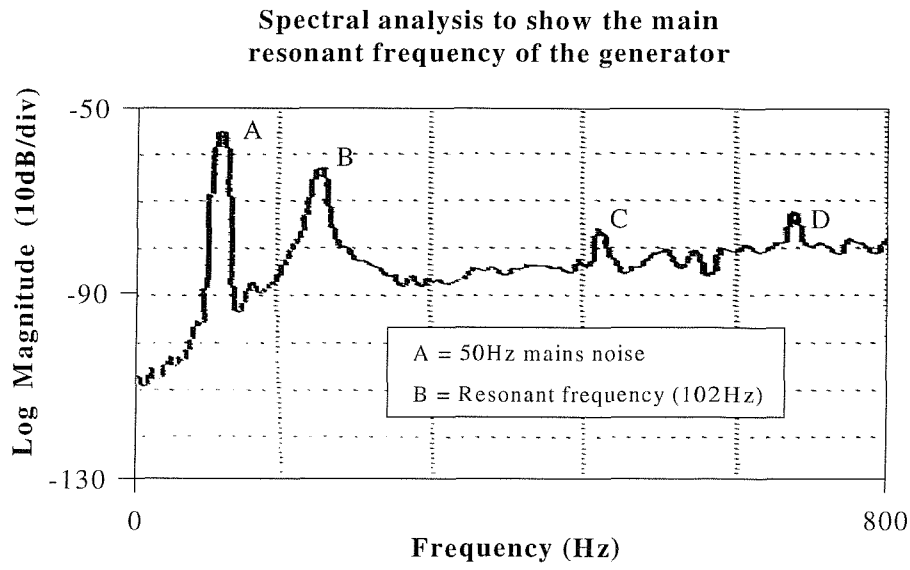

Figure 11: *Determination of the generators main resonant frequency*

4.3 Choice of transformer

The micro power generator, shaken at 102Hz with an amplitude of 0.4mm, produces a voltage of approximately 0.5V. This is too low for its output to be rectified directly using silicon diodes where the forward voltage needs to be at least 0.6V. For efficient rectification it is desirable for the voltage to be much greater than a diode forward voltage to make switching losses less significant (at least an order of magnitude). At the very least, the voltage must exceed the diode forward voltage for the system to function. One method of stepping up the voltage is to use a transformer.

The transformer needs to be as energy efficient as possible and it must satisfy the following design considerations.

- A turns ratio that can step the generated voltage up to approximately 3V. Given the typical output voltage from the generator of about 0.5 volts, a step up ratio of at least about 5 is required.
- An input impedance that is matched to the generator's output impedance at the generator's operational frequency. This is to satisfy the condition of maximum power transfer. At 100Hz this is a value of about 121Ω.
- An output impedance that is matched to the rectifier input impedance. This is also required to ensure that the condition for maximum power transfer is

achieved. The rectifier input impedance is dependant on the current used by the SPMS. For this specific example the input impedance is approximately 100kΩ (dependant partly on the number of digits energised on the display).

- The transformer needs to be able to handle the current produced by the generator. Given that the current is likely to be very low (less than about 2mA) this should not be a significant issue.
- The transformer needs to have good coupling between the primary and secondary coils at the operational frequency of the generator. This will require the use of a suitable core.

Two different core materials, iron-based and ferrite have been evaluated for inclusion in the magnetic path of the transformer. These materials have increased permeability (with respect to air) which improves the magnetic flux density and therefore the efficiency of the transformer. The ferrite material was discounted because at the desired frequency of operation (≈100Hz) the material provides no benefit. Iron, on the other hand, does provide an improvement in efficiency even at low frequencies. One disadvantage is, however, that most transformers utilizing iron cores are relatively large compared to the typical size of other components within the SPMS. Another consideration is the impedance of the transformer which has to be well matched to both its source and its load for maximum power transfer.

Equation 1 (for an ideal transformer) can be used to calculate the turns ratio that will ensure maximum power transfer from the generator into the SPMS. This equation does not take into account the consideration of stepping up the voltage produced by the generator for ease of rectification.

$$\sqrt{\frac{Z_{gen}}{Z_{spms}}} = N:1 \qquad (1)$$

For the demonstrator system detailed here, optimizing the impedance match results in a transformer with a step up ratio ≈3.1. However, for efficient rectification a greater step up ratio is required. Optimum power transfer including rectifier efficiency, occurs with a ratio between 5 and 10. A ratio of 7 has been used in the demonstrator system. Figure 12 shows a model of the transformer matching circuit.

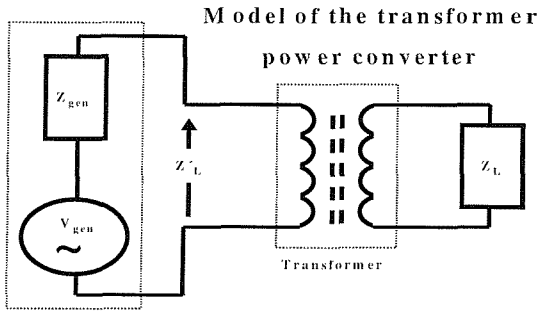

Figure 12: *Model of the transformer impedance matching circuit*

The power, P_L, going into the SPMS from the transformer secondary winding (for the matched, ideal transformer case described in equation 1) can be calculated using equation 2, where Z'_L is the load as seen by the generator.

$$P_L = I_1^2 Z_L = \left(\frac{V_{gen}}{Z_{gen} + Z'_L} \right)^2 Z'_L \qquad (2)$$

The voltage produced by the generator is dependant on the amplitude of the vibration. A displacement of the magnet of 0.4mm at the generator fundamental frequency of 102Hz produces approximately $0.5V_{rms}$ and a constant power of 1.25mW.

Table 1 lists the transformer parameters. Figure 13 show the efficiency for three transformers that were evaluated in the SPMS. Transformer A was chosen for the final demonstrator as it was able to maintain its efficiency at power below 1mW and it was the smallest (in physical terms) of the transformers tested.

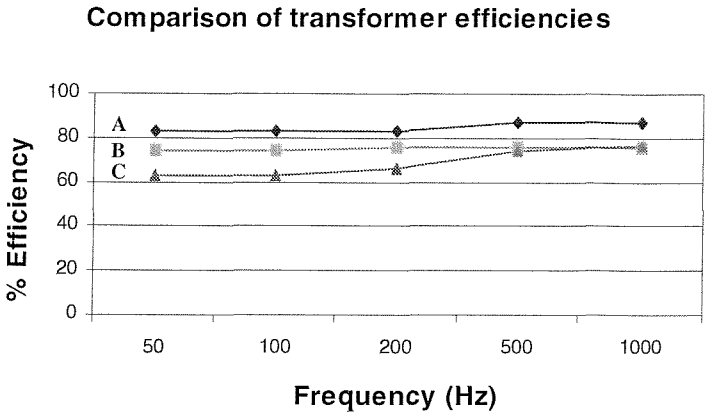

Figure 13: *Efficiency at a range of frequencies for three sample transformers (at 1mW power output)*

Transformer	Primary Ω	Secondary Ω	Ratio
A	600	20k	1:7
B	150	600	1:5
C	22	150	1:10

Table 6: *Test transformer parameters*

4.4 Choice of rectifier

Rectification is not a trivial issue when the voltage to be rectified is comparable to a diode turn on voltage, but schottky diodes (for example the BAT54J used here) can help to reduce the losses due to forward conduction (that can be modeled as a non-zero series resistor). Switching losses as a result of the diodes' reverse recovery time have been reduced in the prototype by choosing a relatively low operational frequency of about 100Hz.

A full bridge circuit has been constructed with four diodes. This is more efficient than just simply using a half wave rectifier, given that energy from the whole waveform cycle is converted by the rectifier. However, this setup has the disadvantage that the internal voltage drop is the forward voltage of two diodes and not one diode. The circuit shown in figure 14 has also been constructed using OA90 signal diodes. These diodes also have a low turn on voltage (compared to silicon) and are also designed for low power operation.

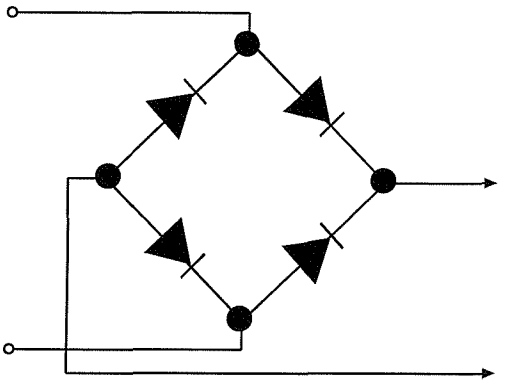

Figure 14: *The full bridge rectifier circuit*

Table 2 and figure 15 show the efficiency of both the full bridge schottky and full bridge signal diode rectifiers (BAT54J and 0A90 respectively) over a range of frequencies. Both rectifiers are suitable for operation with the SPMS. The schottky based rectifier was used for this demonstrator.

Freq. In	In (mA)	In (mW)	Out (mA)	Out (V)	Out (mW)	Efficiency %
50	2.9	8.7	2.68	2.66	7.1	82
100	2.9	8.7	2.63	2.66	7	81
150	3	9	2.7	2.66	7.2	80
200	3.1	9.3	2.7	2.66	7.25	78
300	3.1	9.3	2.7	2.64	7.16	77
500	3.2	9.6	2.8	2.64	7.3	76
For Schottky diode devices at 3V p-p input and a load of 1k Ohm						

Table 7: *Results for Schottky diode rectifier efficiency*

The results in table 7 imply that the higher the frequency of operation, the lower the rectifier efficiency. When considering the overall efficiency of the system, however, there is a trade off between the transformer efficiency and the rectifier efficiency. For the demonstrator the choice of operational frequency was determined partly by the vibration generator design and partly by a desire to operate at a frequency that was

known to have potential applications. It was therefore decided that 100Hz was a suitable frequency of operation for the demonstrator.

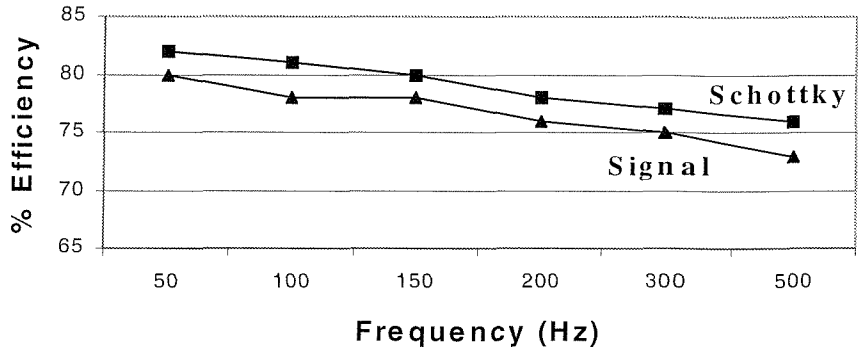

Figure 15: *Measured efficiency of Schottky and signal diode full bridge rectifiers*

4.5 Regulation of the power supply

The generated power needs to be voltage regulated to ensure the voltage supplied to the SPMS circuit is kept within the operational range for all devices (3V to 5V). Voltage regulation can also reduce unwanted noise that is present at the generator's operational frequency.

The Maxim range of DC to DC converters are suitable for this application because they are able to operate at low power (μW) with a high level of efficiency. Several devices were evaluated as shown in table 3, however the MAX 1672 and the MAX 1725 were ruled out initially due to their requirement for a relatively high input voltage when compared to the MAX 1722 and the MAX 1723. The MAX 1672 was also ruled out because of its high quiescent supply current.

Parameter	MAX 1672	MAX 1722	MAX 1723	MAX 1725
Input voltage range	1.8V to 11V	0.8V to 5.5V	0.8V to 5.5V	2.5V to 12V
Quiescent supply current	85µA	1.5 µA	1.5µA	2µA
Output voltage	3.3V	2.7V to 5V	2.7V to 5V	1.5V to 5V
Complexity/size of associated circuit	Average	Average	Average	Average
Has LX damping	No	Yes	No	No
Has shutdown mode	No	No	Yes	Yes

Table 8: *Comparison of four viable DC/DC converters*

Both the MAX 1722 and the MAX 1723 require a similar setup circuit. For the circuit shown in figure 16, L1 is 10mH and both capacitors are 100µF. The potential divider values are chosen such that the output has 3.6V and the feedback pin (FB) has 1.235V. The FB pin has a leakage of 20nA (max), hence the resistor values should be in the region of 100k Ohm to 1M Ohm.

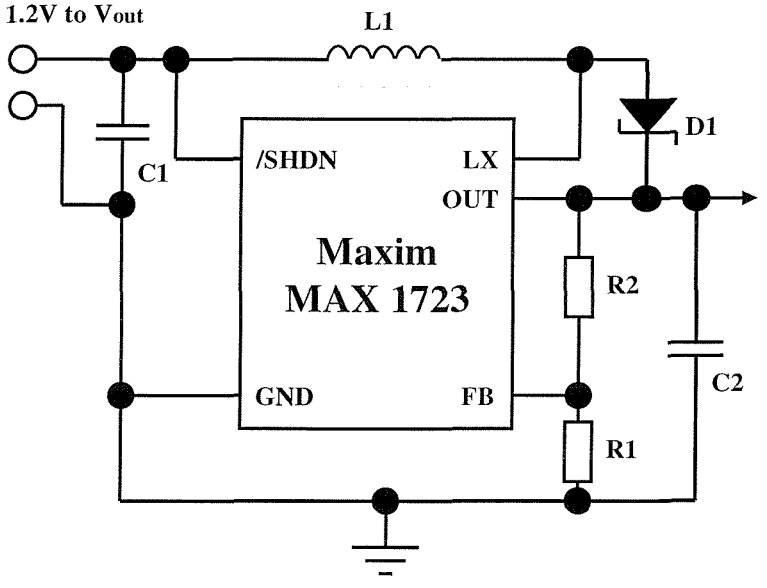

Figure 16: *The DC/DC test circuit without a load*

There is little to choose between the MAX 1722 and the MAX 1723. Experimental work has shown that the MAX 1723 functions in the SPMS circuit but does result in noise at the rectifier output and this is degrading the operation of the rectifier, even with the addition of an appropriate capacitor at the rectifier output. The MAX 1722 has LX damping. This is simply additional built-in circuitry to reduce the voltage spikes caused by the DC/DC internal switching circuitry. Such voltage spikes can be seen on both the DC/DC converters input and output on other models. For this application such damping is beneficial. Figures 17 and 18 show that there is still switching noise, even with the LX damping.

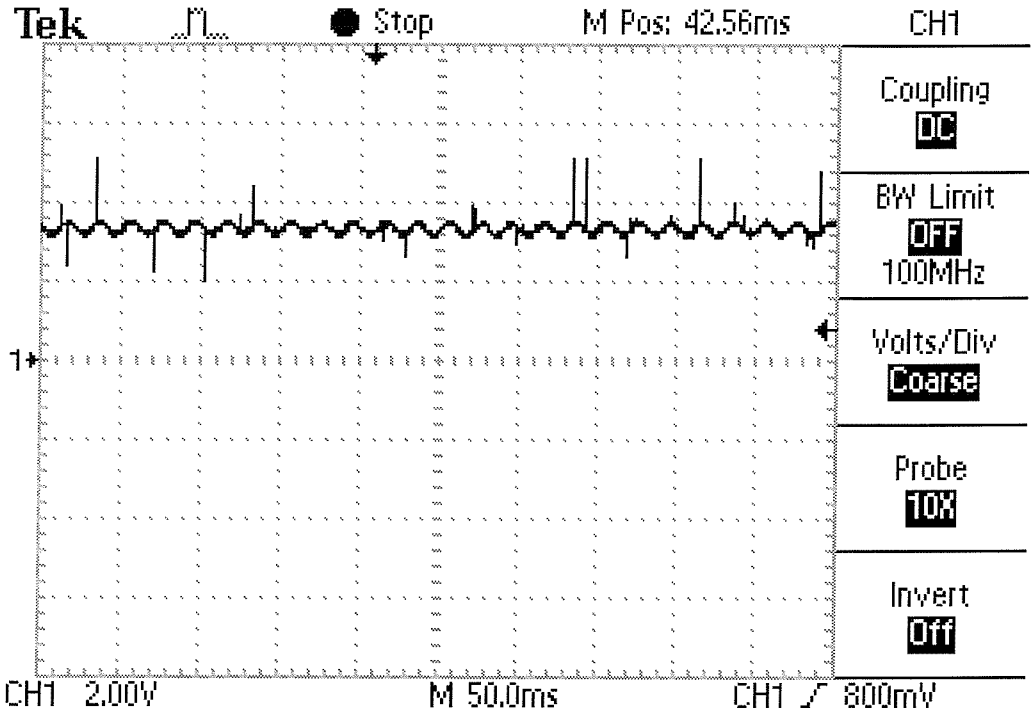

Figure 17: *MAX 1722 DC/DC converter output voltage with a 10k Ohm load*

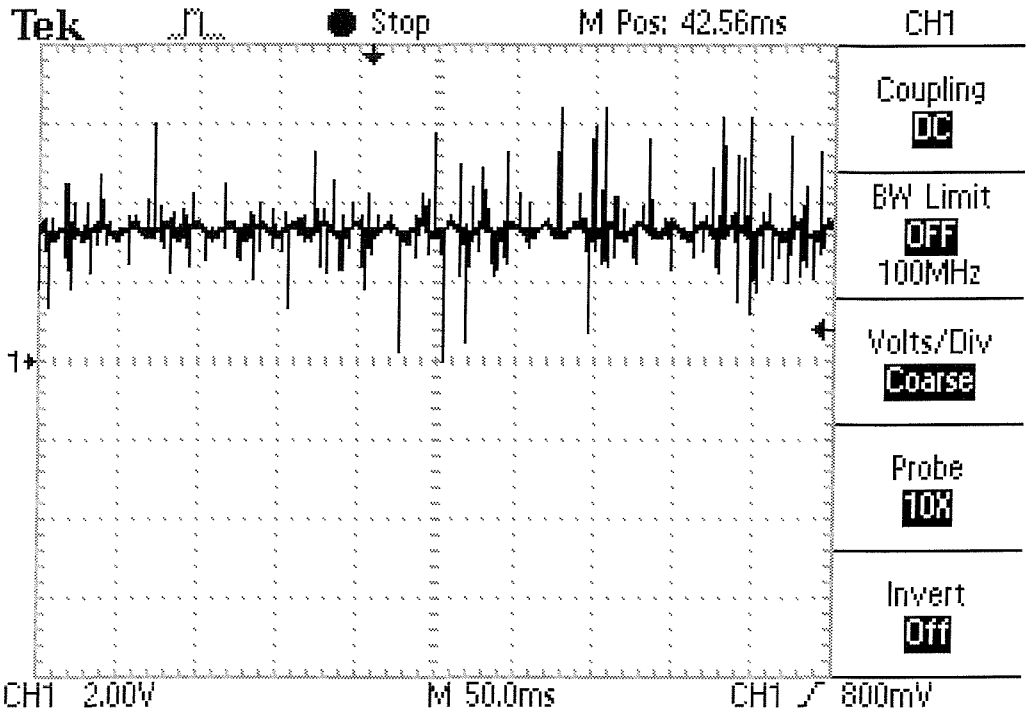

Figure 18: *MAX 1722 DC/DC converter output voltage with a 1k Ohm load*

Table 4 shows the levels of efficiency for the Max1722 converter. These initial values of efficiency have been calculated using a digital volt meter (DVM) with the assumption that the waveform is DC, however it seems that the waveform (both input and output) may have some significant frequency components.

Input	Output	Efficiency
1.2V	3.35V	
6.0mA	0.34mA	
7.2mW	1.14mW	15.80%
1.4V	3.35V	
5.31mA	0.34mA	
7.4mW	1.14mW	15.40%
1.60V	3.50V	
4.00mA	0.35mA	
6.4mW	0.12mW	19.20%
1.8V	3.37V	
3.61mA	0.34mA	
6.50mW	1.15mW	17.69%
2V	3.39V	
4.0mA	0.34mA	
8.0mW	1.15mW	14%

Table 9: *Measured values of efficiency for the 1722 DC/DC converter.*

Figures 17 and 18 show how, as with all the DC/DC converters tested, as the output is loaded the regulation goes down. Given a combination of this factor and the low efficiency measured, an alternative zener diode regulator was used in the demonstrator.

The efficiency of the zener diode was kept as high as possible by operating it close to the non-linear region of its characteristics. This is possible because, during normal operation the current used by the SPMS is constant to within 8%. It was found that a 4V7 zener diode could regulate the supply well at just over 3V. The main change in current occurs as the LCD changes value. The efficiency of the zener diode regulator is typically between 80 and 84%.

4.6 Choice of sensor

For the initial demonstrator system, a low power sensor with respect to the overall power available within the system (about 1μW) and suitable for use in real life applications was required.

A search identified a range of potential sensors and two sensors were identified for consideration.

- The SP13 pressure sensor made by SensNor™
- The Analog Devices™ accelerometer model ADXL202

The SP13 pressure sensor is a suitable candidate because it is designed to operate on 3V and could operate well within the available amount of power. However, we were not able to obtain a data sheet from the manufactures for this device so it was discounted.

The Analog Devices™ accelerometer operates within the ±2g range and has been used as the sensor for this demonstrator. The accelerometer has a bandwidth that can be set (using external capacitors) from 0.01Hz to 5kHz. The accelerometer produces a PWM output. This output can be put through a low pass filter (comprising a resistor and a capacitor) to produce a DC voltage that relates to the inclination of the accelerometer. The ADXL202 is a dual axis device, however for the demonstrator described in this chapter only one axis needs to be used. This type of sensor would be suitable for condition monitoring applications.

4.7 Choice of display

The micro-system needs to communicate data from the sensor to its external environment. This can potentially be a power hungry process, hence it is important to choose a technology that is appropriate, both in terms of usability for the given application and power consumption.

This demonstrator system described here uses a low power liquid crystal display to communicate the sensors readings. A search for low power displays was made and two displays (made by Lascare electronics) were identified, the DPM 702S and the DPM 1S-BL.

The DPM 702S requires about 2.1mW for operation (without its backlight) and the DPM 1S-BL required about 750μW for operation. Since the DPM 1S-BL uses less power it was decided that this device should be used in the first prototype micro-system. The circuit diagram being used is shown in figure 19.

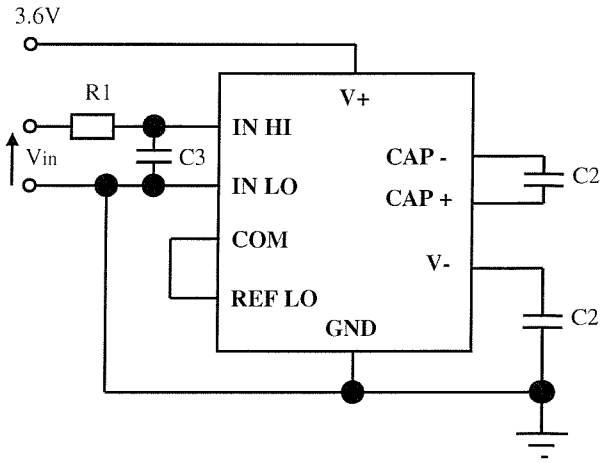

Figure 19: *Circuit diagram for the DPM 1S-BL display module*

The value of R1 is 1MΩ, the values of C1 and C2 are 1μF and C3 is 10nF.

Figure 20 shows the circuit used to interface the accelerometer output with the display circuit. The display requires an input that has a magnitude of less than 200mV. The circuit in figure 12 both converts the voltage down to a suitable level and it acts as a low pass filter to convert the PWM accelerometer output into a dc voltage. The negative power rail is generated by the display circuit and has been used to ensure that the display reading is fixed about a value of zero for the mark to space ratio associated with an accelerometer tilt of zero degrees.

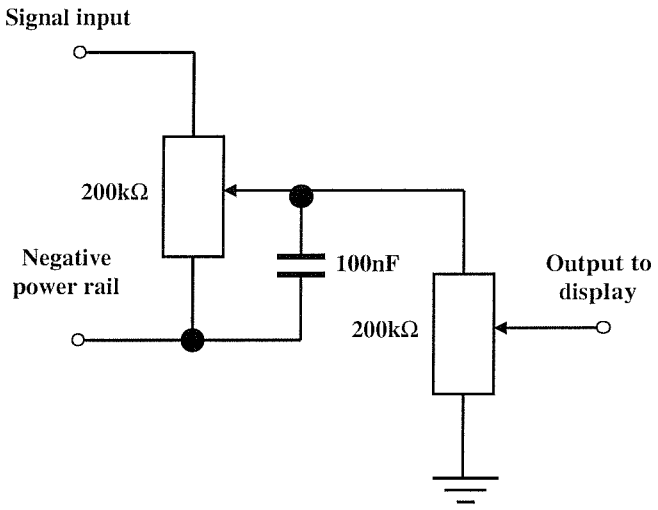

Figure 20: *Circuit to interface the accelerometer to the display circuit*

4.8 Micro-System Layout

Figure 21 shows the prototype SPMS layout. The components as shown are 1) generator input 2) step up transformer 3) the rectifier 4) regulation circuitry 5) accelerometer control circuitry 6) the accelerometer 7) display control circuitry 8) the display connector.

This layout was chosen to keep the ac power and the dc signal components as far apart as possible. For stable operation of the accelerometer the capacitors associated with the device also needed to be in close proximity.

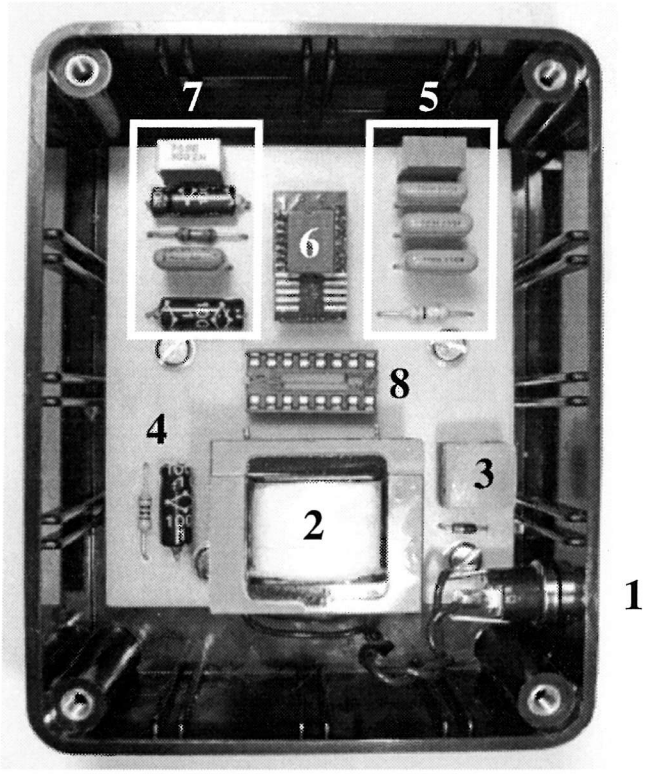

Figure 21: *A prototype SPMS that uses an LCD display to communicate the reading from a sensor*

4.9 Calculating the forces applied to the generator by the shaker rig

The minimum force that the shaker rig has to apply to the SPMS for reliable operation has been measured using an accelerometer (ADXL202) that has a 2g range.

First the accelerometer was calibrated. This was done by taking a reading of its Pulse Width Modulation (PWM) output duty cycle at two angles 180 degrees apart. This represented a change of 2g.

Measured PWM output with the diaphragm parallel to the force of gravity:

Mark = 416μs, Space = 292μs ... therefore the duty cycle is 58.76%

Measured PWM output with the diaphragm 180% to above:
Mark = 248μs, Space = 468μs ... therefore the duty cycle is 34.64%

We can therefore say that a change in applied force of 2g produced a change in the PWM waveform of 24.12% and an applied force of 1g would produce a change in the PWM waveform of 12.06%. For a constant frequency (of 1.4kHz) the percentage change of the PWM output is linear with force (provided the force is within the accelerometer's 2g range).

To calculate the forces being applied by the shaker rig the accelerometer was connected to the rig while it was shaking and the two directional acceleration readings were made.

For an upward motion of the shaker rig:
Mark = 400, Space =316 ... therefore the duty cycle is 55.87%

For a downward motion of the shaker rig:
Mark = 436, Space = 272 ... therefore the duty cycle is 61.59%

From this the g being created by the shaker rig can be calculated:
58.76% - 55.87% = 2.89% ... this equates to 0.24g
58.76% - 61.59% = -2.83% ... this equates to -0.23g

4.10 Summary of results

It has been shown that a LCD based SPMS (measuring just 75 x 100 x 40mm) can operate continuously from the micro-generator described that produces just under 1mW. This demonstrator is able to function with a force (external to the generator) of just 0.23g at a frequency of 102Hz. The SPMS is able to continuously display a number on its LCD that relates to the measurement on an accelerometer. The maximum sensitivity of the demonstrator SPMS is 2mg. A reading of 500 on the

display relates to a 1g measurement and a reading of –500 relates to –1g. At present the sensitivity is limited by small fluctuations in voltage after regulation.

4.11 Conclusion

In its present form the SPMS if fully functional, however there are a number of improvements that can be made to address a range of issues like size, power consumption, mode of communication, reliability and weight.

The minimum force required for the SPMS to operate could be reduced by using a power control circuit. This could be a Programmable Interrupt Controller (PIC) that has two key functions. To provide a soft start for the circuit, thus preventing a turn on power surge and to turn blocks of the circuit on and off as required. For the specific demonstrator described in this chapter, a PIC could be used to power manage the accelerometer and the LCD display. For future demonstrators it would also be possible to use a PIC to pre-process data or control communication.

One significant limitation of this demonstrator is the need to view a display that is based on the SPMS. For most real life applications it would be better to have a different method of communication. Infra-red and radio solutions are just two approaches that would potentially create a more versatile system.

The transformer is the largest (and heaviest) system component at the moment and as such it would be sensible to investigate suitable alternative methods of stepping up the generated voltage to a useable voltage of about 3V.

Chapter 5

5. Development of an Infrared Based Demonstrator

5.1 Introduction

This chapter details the design and development of the second self-powered micro-system. The system is once again powered via a magnet-coil generator, as used in the first LCD based demonstrator. The aim of this work is to prove that a self powered micro-system utilising Infra-red (IR) as a method of communication with a remote reader circuit is possible. Furthermore this work aims to detail the main challenges that need to be addressed for such a demonstrator to operate. The hardware described in this chapter is split into two sections, the self-powered micro-system and its associated IR decoder system.

5.2 System block diagram

Figure 22 shows a block diagram for the complete system. The micro-system obtains all of its power from the magnet-coil generator, but the decoder system is powered from an external source. In real life this external source could be a mains power supply or a battery.

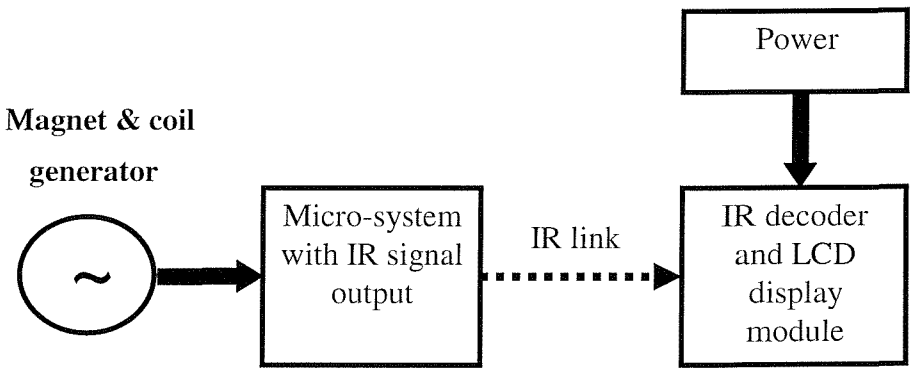

Figure 22: *Block diagram of the SPMS and its associated IR decoder*

5.3 Infra-red based micro-system

This micro-system has five main blocks, the magnet-coil generator, a circuit to step up the generators output voltage and provide rectification, a regulator, the sensor and

the IR transmitter. The block diagram is shown in figure 23. The magnet-coil, the voltage regulation and the sensor are the same as in demonstrator 1. The circuit used to step up the generators output voltage is very different to the first demonstrator, indeed a transformer has no longer been used, but a diode-capacitor combination that is also able to provide the rectification. The LCD in demonstrator 1 has been replaced by an Infra-red emitter on this demonstrator.

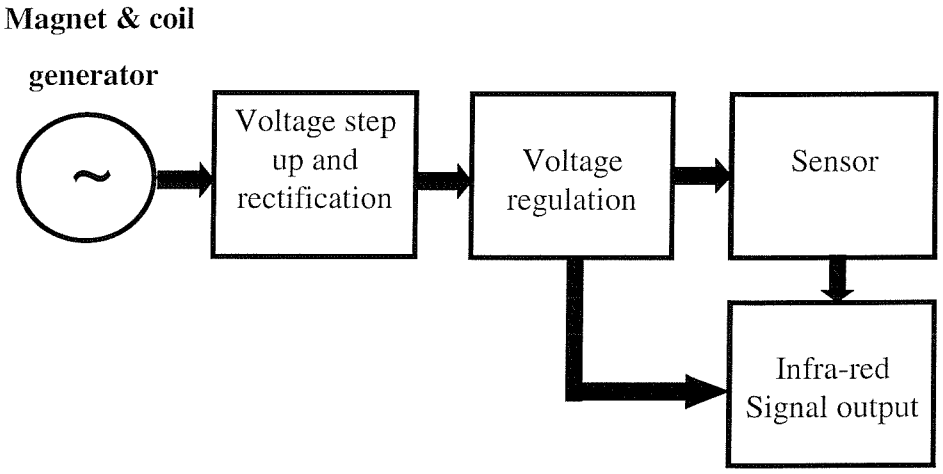

Figure 23: *Block diagram of the SPMS*

2.1 Rectification of the micro-generator output

The SPMS circuit requires a regulated voltage of about 3V, but the generator does not provide a voltage that high and its output is ac, hence the need for a circuit to step up the generated voltage and rectify it. In the LCD based demonstrator this was achieved by using a step-up transformer and schottky diodes to rectify the output of the transformer. This is not ideal because transformers tend to be components that are both large and heavy. Such physical attributes will limit the number of potential applications for the SPMS, hence a new approach has been applied on this demonstrator.

Figures 24 to 26 show some example circuits that are able to both step up an ac voltage and rectify it without the need of a transformer. All of the circuits shown here require the input voltage to be larger than the forward turn on voltage for the diodes used. This is a disadvantage when compared with a transformer, however by using schottky diodes, such circuits are able to operate reliably with the magnet-coil generator.

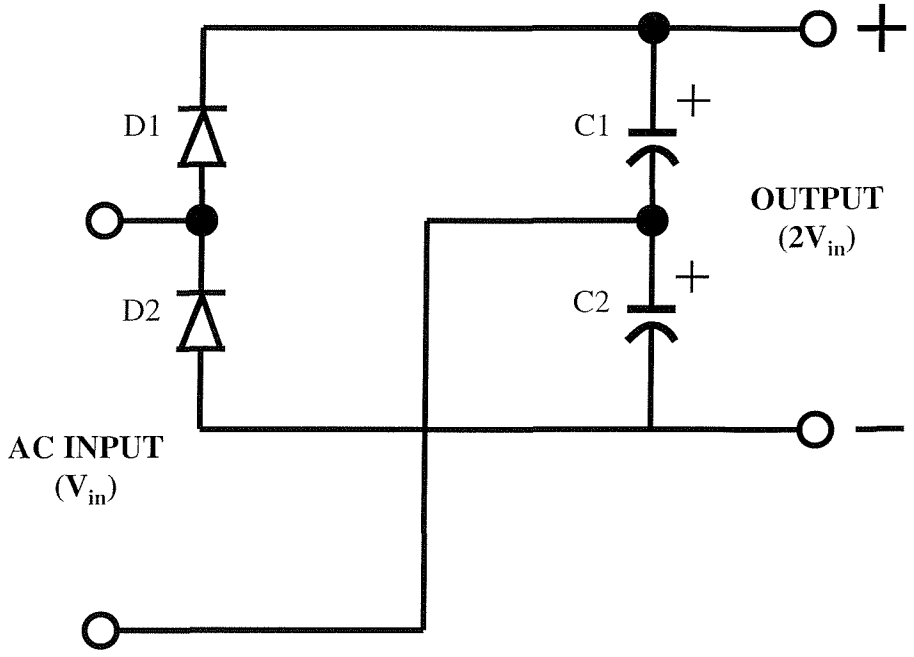

Figure 24: *A conventional voltage doubler*

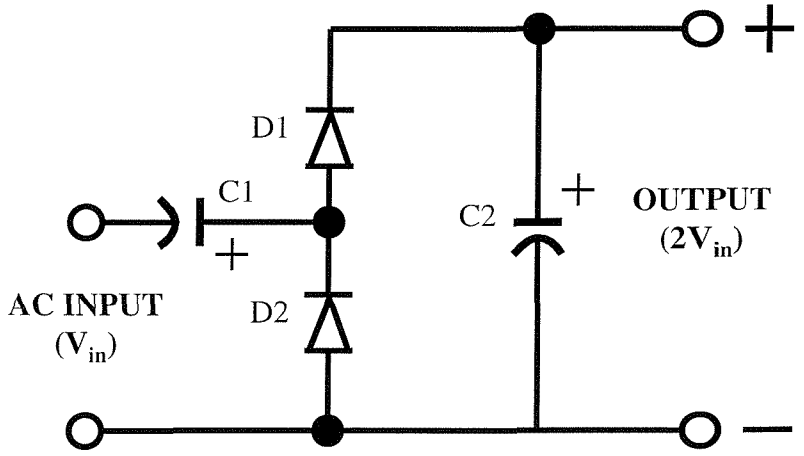

Figure 25: *A cascade voltage doubler*

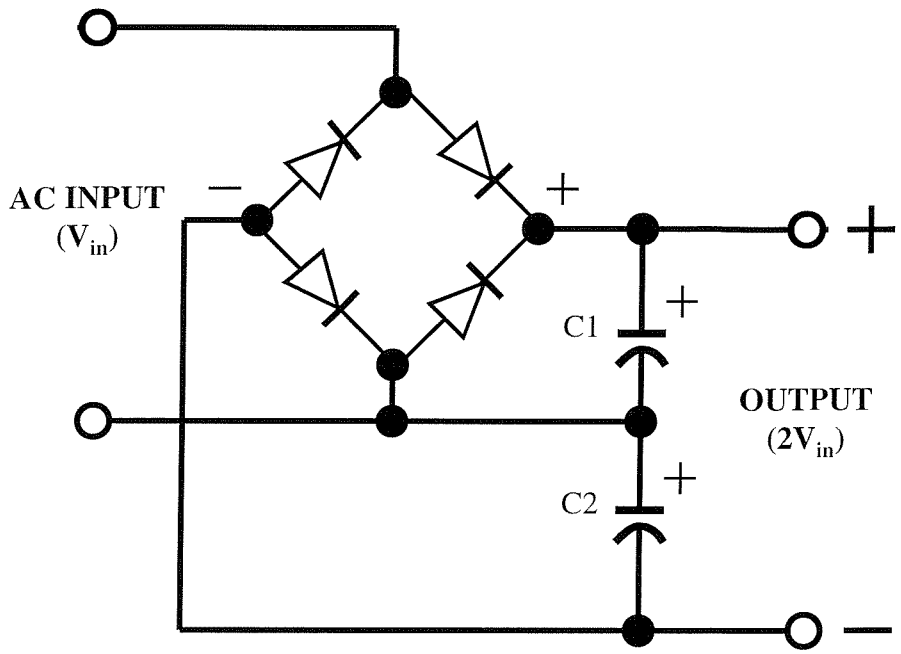

Figure 26: *An efficient bridge voltage doubler*

For this demonstrator system the circuit in figure 27 has been used. This circuit is able to step up the magnet-coil output voltage numerous times as it is not just a voltage doubler. For the SPMS to function a step up of at least 4 is required, else the voltage is too low for the sensor to function.

The minimum value of capacitor used is mainly dependant on the amount of current required by the sensor and IR communication circuit. The capacitors need to store enough charge for continuous operation of the circuit. The voltage at the output of this circuit has been limited by a zener diode regulator, but the regulator does not have a significant voltage drop across it, as this would reduce overall efficiency. Tantalum capacitors have been used in this demonstrator because they are efficient for their size.

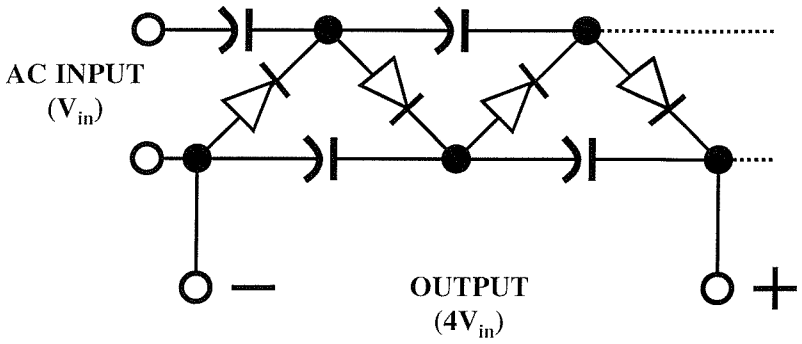

Figure 27: *A generic cascade multiplier*

5.4 Spice simulation of the rectifier

Figure 28 shows the results of a simulation for the four stage voltage step up circuit (the top trace) with no load. A simulation for the same circuit with only two stages is also shown (the lower trace). It can be seen that a finite amount of time is required for both circuits to provide stable output voltages, due to the capacitors.

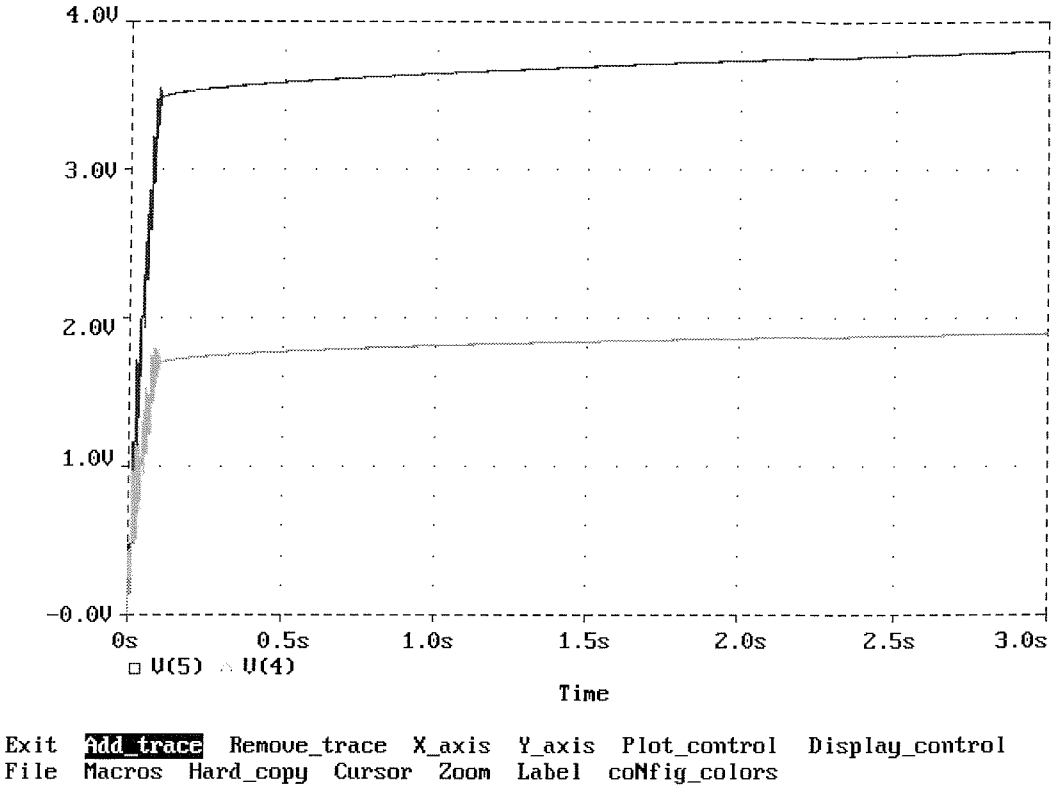

Figure 28: *Spice simulation of a two stage and a four stage voltage doubler*

5.5 Micro-system Regulation

The regulator used for this demonstrator is based upon a 3V3 zener diode. This has been put in series with a resistor across the output of the step-up circuit as shown in figure 8. The zener diode has been designed to operate with a reverse voltage that is only just into its reverse (linear) characteristics. Movement up and down the diodes reverse roll off characteristics is inevitable due to fluctuations in the amount of current used by the demonstrator. The LCD display used in the first demonstrator did not cause significant fluctuations in current, however the infra-red emitter in this demonstrator does cause variations in current that are significant when compared to the overall current being drawn by the SPMS. This could be compensated for, however such compensation was not required for the final demonstrator, as a regulation capacitor was able to provide enough system stability.

5.6 Circuit diagram of the micro-system

Figure 29 shows the final circuit diagram for the infra-red based SPMS. The 22μF capacitors are used to step up the generated voltage, the 48μF capacitor is used to

regulate the power supply. The largest component of the SPMS (excluding the magnet-coil generator) is the sensor.

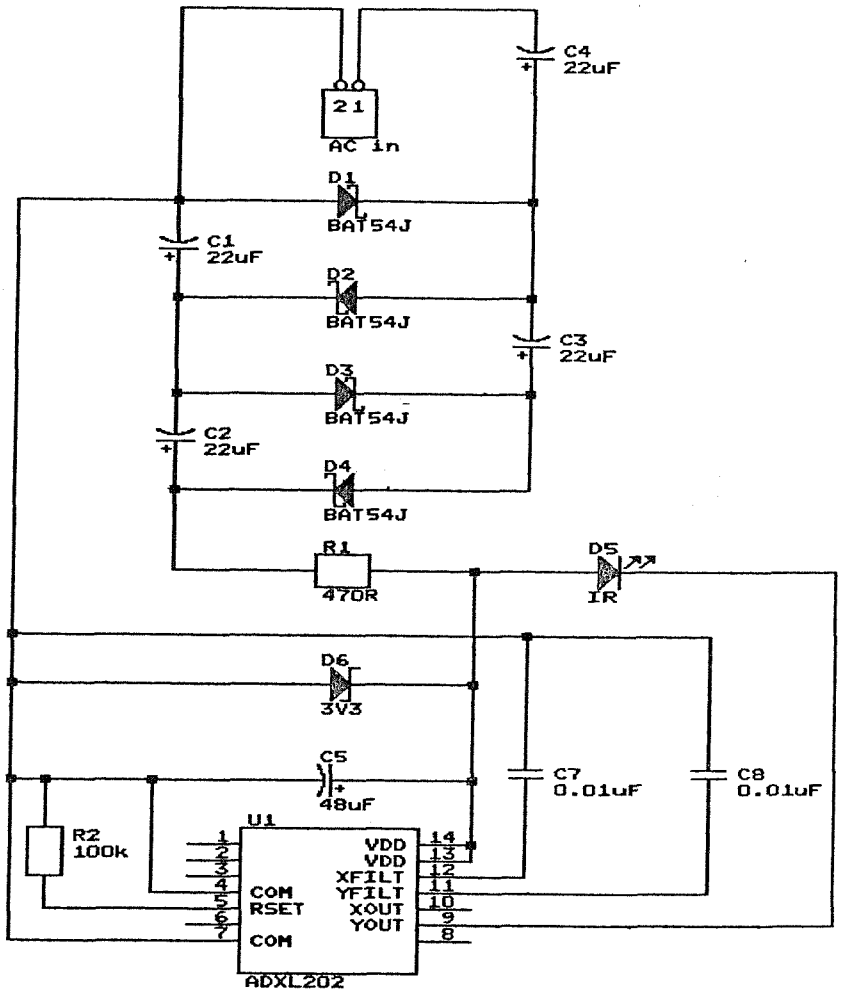

Figure 29: *Circuit diagram of the micro-system*

5.7 Existing methods of IR communication

These days numerous devices use IR as a communication technology and over recent years some standards have been developed, for example, RedRat2 for IR remote controls. The technology used within an IR remote control is comparable to that required by a SPMS. This is because both such systems benefit from being designed to make effective use of available power and transmission distance of a remote control is also similar to the potential distance of operation required by a SPMS. The IR wavelength used in remote controls is often around 1000nm. The standard is to use amplitude modulation of a bit stream using a carrier frequency somewhere around

40kHz. As the signal is a bit stream the amplitude of the carrier frequency is either maximum or nothing.

Once the physical transmission of information is in place, the signal coding is the next level of detail. There are a few standards, such as the Philips RC5 code form, but most manufactures tend to implement their own coding. Modern IrDA technology operates at 4Mbit/s over a distance of about one metre or less. This can be put in context with Bluetooth operating at just 1Mbit/s, but over a range of up to 10m.

5.8 IR transmission using PWM

The output from the sensor is in a PWM format and this PWM signal has been sent directly to the infra-red emitter on the SPMS. To reduce the amount of power used by the infra-red emitter this signal could be fm modulated, however this would require additional circuitry that would also require power. It is envisaged that a low power PIC could be used to power manage the SPMS, however the aim of this demonstrator is to prove that an infra-red micro-system is simply viable soution.

5.9 Micro-system hardware

The micro-system hardware is shown in figure 30. Some of the components that are surface mount have been mounted within an encapsulated package to protect them. The four step-up capacitors and the regulation capacitor can be seen in figure 30. It can be seen that the overall size reduction compared to the LCD based generator is significant.

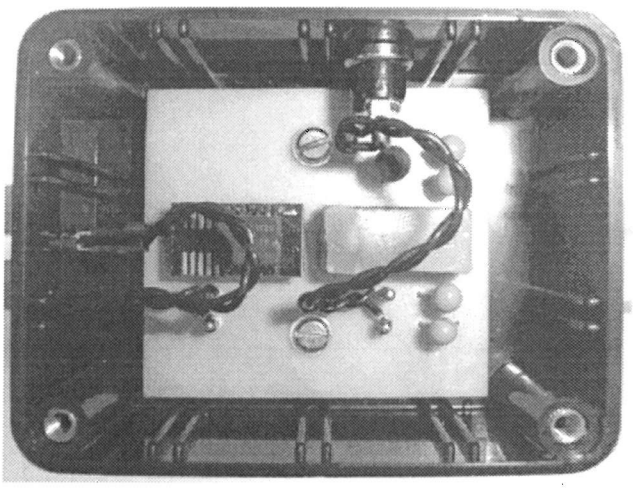

Figure 30: *The final SPMS (excluding the magnet-coil generator)*

5.10 Infra-red signal decoder

5.10.1 Overview of the decoder

The decoder block diagram is shown in figure 31. The aim of this circuit is to re-construct the PWM signal being sent by the SPMS. This is achieved by amplifying the received infra-red signal and then using a comparator to re-construct the square wave.

Once the PWM signal has been re-constructed it is sent into a low pass filter to produce a dc voltage that is compatible with the display module. Both the filter and the display circuit were present in the first demonstrator, but now they are no longer part of the SPMS. The display now forms part of a system that is remote to the SPMS, hence there is no power limitation.

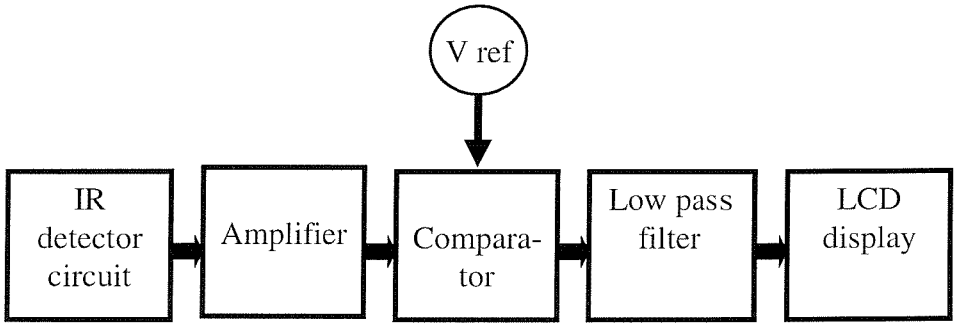

Figure 31: *Block diagram for the decoder*

5.10.2 Circuit diagram of the decoder

Figure 32 shows a circuit diagram of the decoder. The system is based around an EL2244CN operational amplifier. This device contains two amplifiers and in this application one of the devices is being used as the voltage comparator.

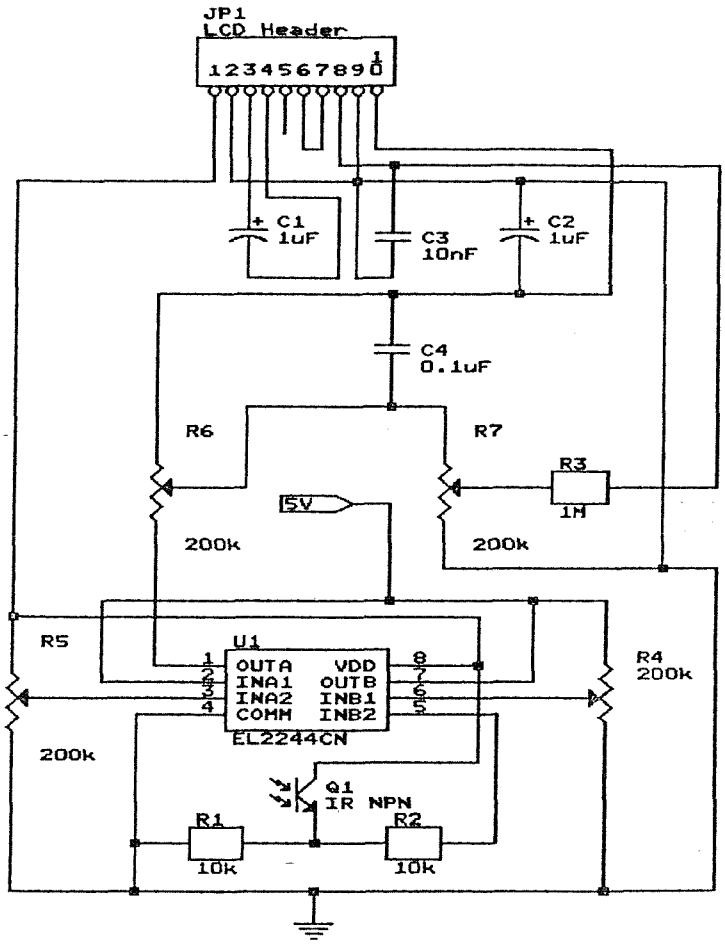

Figure 32: *Circuit diagram for the IR decoder*

5.10.4 Calibrating the decoder

The decoder has been calibrated (using the potentiometers shown in figure 12) to provide the same accuracy as the LCD based demonstrators.

5.10.5 Ways to improve the decoder

It has been found that the IR emitter used in this prototype does not have enough power available to turn on and off with an insignificant rise and fall time. As a result this demonstrator transmits a PWM waveform that has a slightly reduced accuracy. The finite amount of time taken for the transmitter pulses to rise and fall cause the

received mark to space ratio to change in relation to the distance between the SPMS and the IR receiver. There are several possible approaches to solving this problem. These are:

- Operate at a fixed distance
- Use a lower power IR LED or power management on the SPMS
- Use gain control at the receiver
- Modulate the transmitted signal at a higher frequency

The use of gain control is possible because the received maximum pulse amplitude is also a function of distance, hence the peak amplitude can be used to compensate for the change in mark to space ratio.

Modulation of the signal at a higher frequency would be compatible with other existing IR communication technology, however this approach would require the SPMS to power an additional oscillator circuit.

The maximum distance of communication could also be increased further by placing a filter over the IR receiver to cut out most of the un-wanted ambient light.

5.10.5 IR Receiver hardware

Figure 33 shows the actual decoder circuit excluding the LCD that is mounted in the case (as shown in figure 34). The hardware has been mounted into a box that is the same size as the SPMS box to ensure alignment of the infra-red emitter and detector on the test rig shown in figure 15. The decoder required a 5V supply to operate.

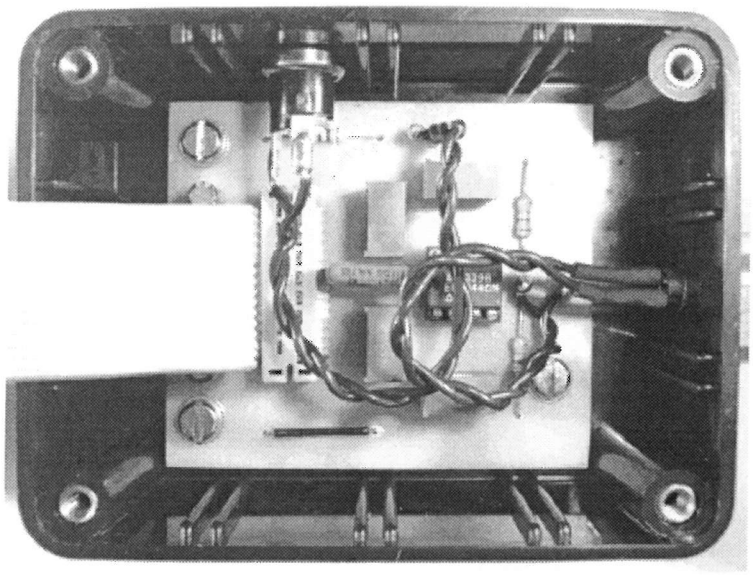

Figure 33: *The final decoder (excluding LCD)*

5.11 System layout

The SPMS and its associated receiver have been mounted on a base that is able to align the infra-red emitter and photo transistor. This base is shown in figure 34. For an application in the field this base would not be required, however for a demonstrator it is useful if the two devices can be placed a known distance apart. Using this configuration the system has been able to operate with a gap in excess of 80mm. The limit of operation is not just limited to the available power at the SPMS, but also the sensitivity of the receiver circuit.

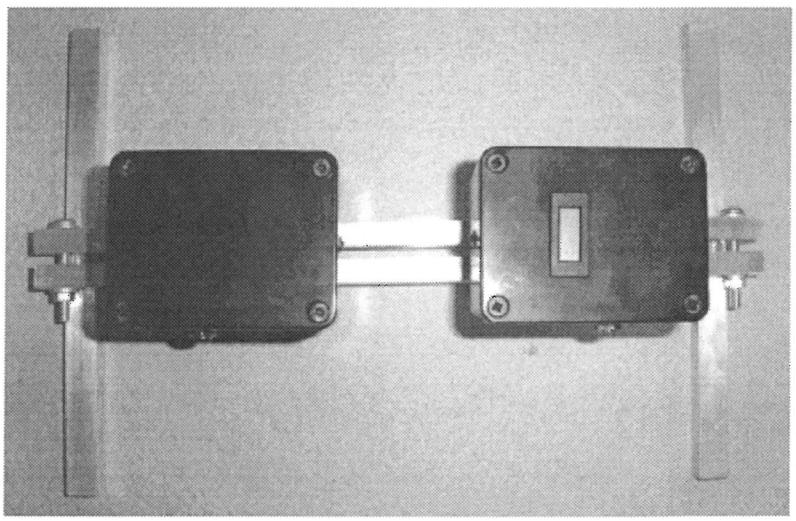

Figure 34: *The complete system with mount*

5.11.1 The linear alignment support mechanism

The two devices (as shown in figure 34) can slide along the base when they are pushed down, but they lock in place when no force is applied. This has been achieved by using a spring mechanism.

5.12 Summary of results

It has been shown that an infra-red SPMS is a viable solution for a SPMS and it has also been shown that using this technology continuous operation is viable, even when there is only about 1mW of power available. The demonstrator in its current form is able to communicate over a distance in excess of 80mm and there is potential for this distance to be increased further without changing the SPMS. This demonstrator is able to function with a force of just 0.23g at a frequency of 102Hz. As with the LCD based demonstrator the maximum sensitivity of this demonstrator is 2mg. A reading of 500 on the display relates to a 1g measurement and a reading of -500 relates to -1g. At present the sensitivity of this system is limited by the process of re-constructing the PWM waveform and errors associated with the additional current required as the IR emitter is energised.

5.13 Discussion of results

Errors relating to the transmission of the PWM waveform can be explained by the SPMS using more power as the mark to space ratio increases. There is enough power for the SPMS to energise the IR emitter constantly, however it can be seen that the SPMS system voltage does fall by about 0.2V as the emitter is energised. This change in system voltage is one on the limiting factors in terms of accuracy of the sensor and amplitude of the transmitted waveform. Given that a finite rise and fall time exists on the PWM signal and any change in amplitude could therefore be seen by the receiver as a change in mark to space ratio. This is an obvious disadvantage of not modulating the transmitted signal and indeed a source of error.

5.14 Conclusion

In its present form the infra-red based SPMS if fully functional and a significant improvement in size has been realised when compared to the LCD based demonstrator. Another significant improvement is with the overall weight of the system. This has been reduced, as a transformer is no longer required. The demonstrator could be improved by using a different communication protocol. PWM is not ideal both in terms of power efficiency and reliability. The diode-capacitor step up circuit has proved to be very reliable and a significant advance on the use of a transformer.

Chapter 6

6. Development of a Planar Coil Micro-System Demonstrator

6.1 Introduction

This chapter details the development of a SPMS that has been designed to communicate via a planar coil. The concept of planar coil communication is not new, indeed it has become common place in RFID tags. It is therefore a proven communication technology that can now be applied to a self-powered sensor-system.

Communication using coils offers many advantages when compared to other forms of communication technologies, such as the optical based solutions described in chapters 4 and 5. Firstly such a micro-system could be fully encapsulated or embedded. This in itself opens up a wide range of potential applications, especially those associated with dirty environments or locations where the sensor-system can not be in a direct line of sight with the receiver/decoder or, in the case of the LCD, the operator. Planar coil technology is also compatible with standard substrate fabrication technology, such as thin or thick-film. It would certainly be feasible for both the sensor and coil to be manufactured on the same substrate using these techniques. This approach has the further benefits of reducing the micro-system size and, potentially, overall production costs.

In this chapter the key formula for communication via planar coil are established and experimental work relating to communication using planar coils is discussed. Planar coils are also presented as a possible alternative to the magnet-coil generator for powering the SPMS.

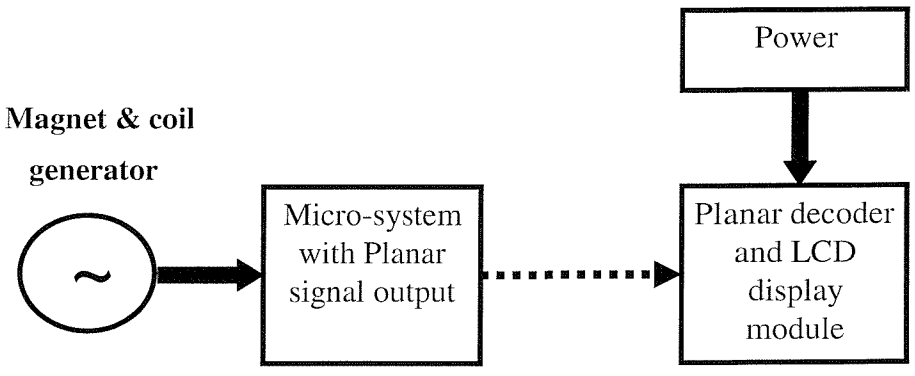

Figure 35: *Block diagram of the SPMS and its associated planar decoder*

Figure 35 shows a block diagram of the planar based sensor-system and its associated receiver/decoder. The magnet-coil generator is the same generator that was used in the previous optical based micro-systems. This generator is once again used to power a sensor-system comprising of power management circuitry, sensor and a planar coil. Figure 35 also shows the decoder and display module. As with the IR receiver this can have its own external power supply as it is remote from the sensor-system. The decoder has been designed to operate within the near field of the sensor-systems planar coil. The function of the decoder is to re-construct the data radiated by the sensor-system and display it on a LCD.

This chapter explores the possibility of operation at a communication frequency of 1.2kHz (as this is the existing data frequency). A higher frequency, in the region of MHz could increase the operational range of the system and it would also enable there to be a significant reduction in physical coil size, however there are other factors to consider, for example the amount of additional energy this higher frequency would require.

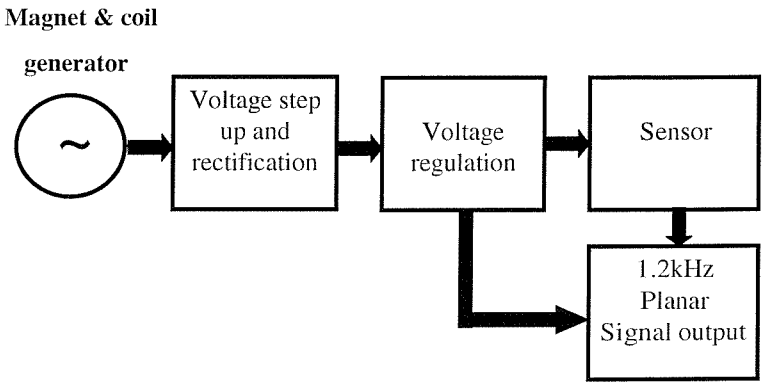

Figure 36: *Block diagram of the SPMS*

Figure 36 shows a block diagram of the prototype micro-system with its associated planar coil interface in more detail. The voltage step-up and rectification block is used to convert the magnet-coil output voltage (<0.5V) up to a higher voltage. This voltage is a volt or so higher then the regulation voltage. The regulation voltage has been set to be 3V. Figure 36 is designed to show the conceptual design of the micro-system.

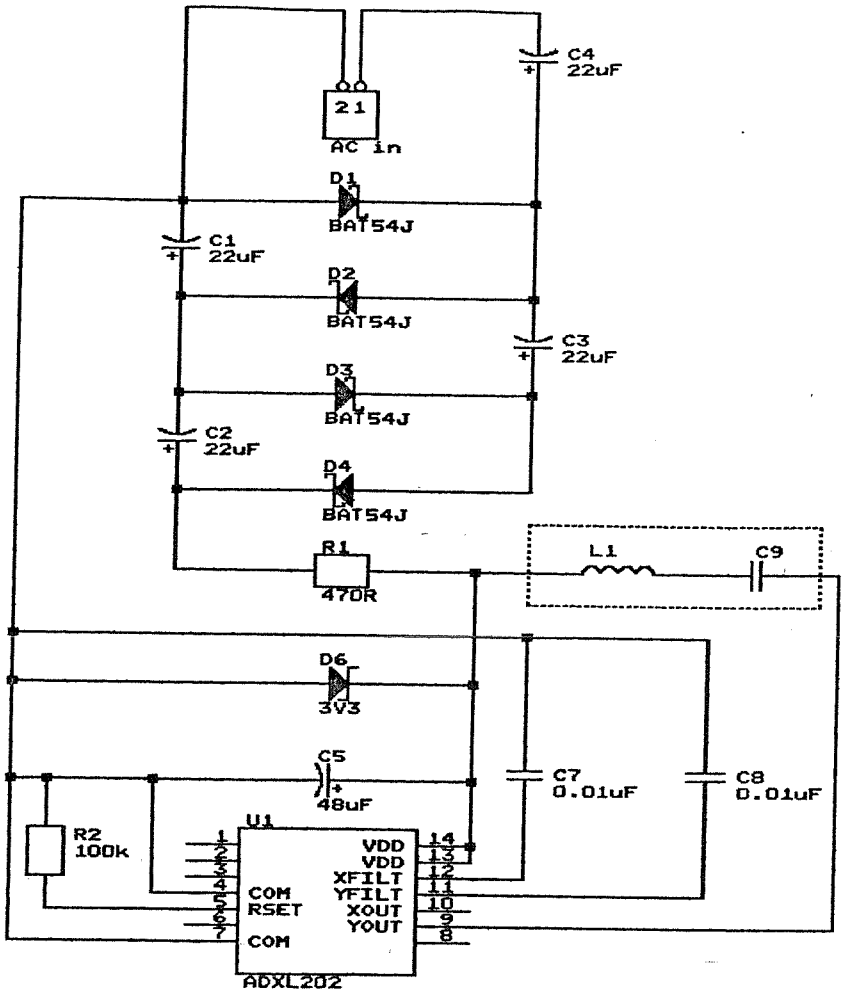

Figure 37: *Circuit diagram of the planar based micro-system*

Figure 37 shows a circuit diagram for the planar based micro-system. The planar coil in this circuit has been designed to operate at resonance and is used to communicate the PWM signal directly from the accelerometer. This approach has the power advantage of not requiring additional circuitry to process the data for transmission, however it has the disadvantage that the communication signal is a square wave. This is a disadvantage because the fourier analysis of a square wave shows that it contains an infinite number of odd harmonics. It is therefore inevitable that a planar coil with a single resonance frequency and a finite bandwidth will distort this waveform. The circuit in figure 37 assumes that there is enough power available for continuous communication via the planar coil. However, this is not the case and therefore the system requires a re-design. Figure 38 shows typical (measured) values of power required by the transmitter coil when operating at 1.2kHz.

6.1.1 Measurement of power required for communication

Although the trend shown in figure 38 looks to be linear (for a constant value of 0.1V across the reception coil), power levels below 5mW are not high enough for the actual transmitter coil used to radiate a measurable electro-magnetic field. At distances over 20mm the power required did not remain linear. Even with 100mW being used by the radiating coil the limit of operation for this system was measured to be 45mm.

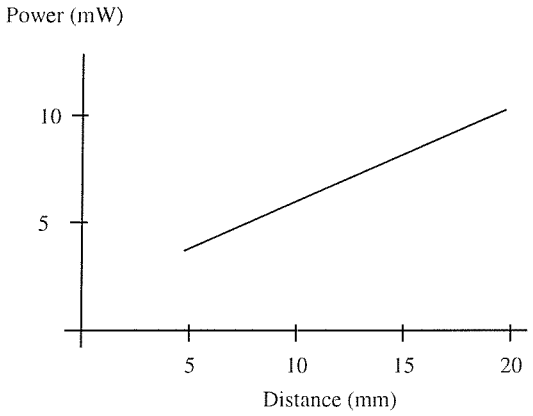

Figure 38: *Power required for signal transmission*

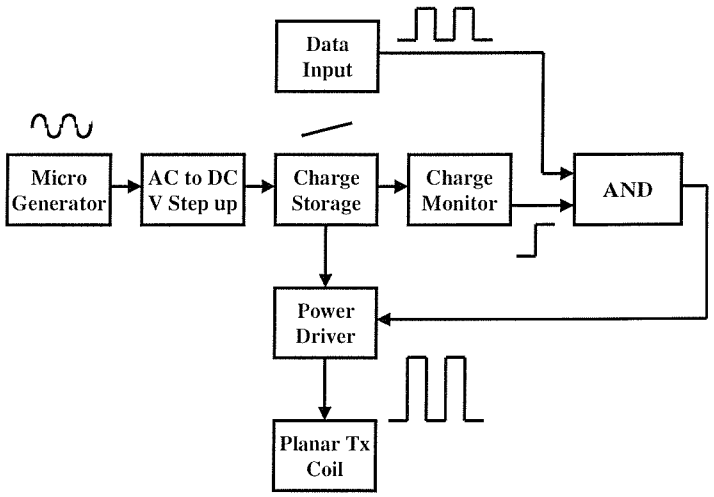

Figure 39: *The final SPMS block diagram*

Figure 39 shows a revised block diagram for the SPMS. This block diagram has the additional blocks to handle both charge storage and power management. The concept is to store charge in a capacitor until there is enough charge for a finite period of

communication. The sensors output forms a data input to the system, as shown on the block diagram. A separate AC to DC step up circuit (not shown on the block diagram) can be used to power the accelerometer. This approach has the advantages of being able to provide a stable power supply for the sensor during periods of transmission via the planar coil. The sensor would also be active all the time, hence there would be no problems associated with bad data integrity at the start of the transmission cycle. This approach does however mean that the standby power when the system is not transmitting is not as low as it could be. For efficient use of available power during communication the voltage given out from the charge storage circuit is about 10V. Experimental work has shown that this is about the minimum voltage required for the planar coil (operating at 1.2kHz) to radiate a useful electromagnetic field.

6.1.2 Design Of The Power Management Circuit

The SPMS described in this chapter is able to operate continuously using just the power produced by the magnet-coil generator. A power management circuit able to provide increased levels of power for a short period of time could be used should it be necessary to increase the distance between the SPMS and the receiver module. The distance can be increased given that more power would be available for the transmitter module to utilize. Such a circuit, as shown in figure 40 has to store power over a period of time. In figure 40 diodes 1 to 8 and capacitors 1 to 8 are all associated with the voltage step up circuit. Capacitor 9 is the main power store. Once a pre-determined voltage (3.6V) is reached the zener diode D9 turns on the transistors base and charges Capacitor 10. Capacitor 10 and resistor 3 then keep the transistor base turned on for a pre-determined amount of time (a few seconds). Once the voltage across capacitor 9 is lower then 3.6V and Capacitor 10 has no remaining charge the transistor turns off and the charging cycle begins once again.

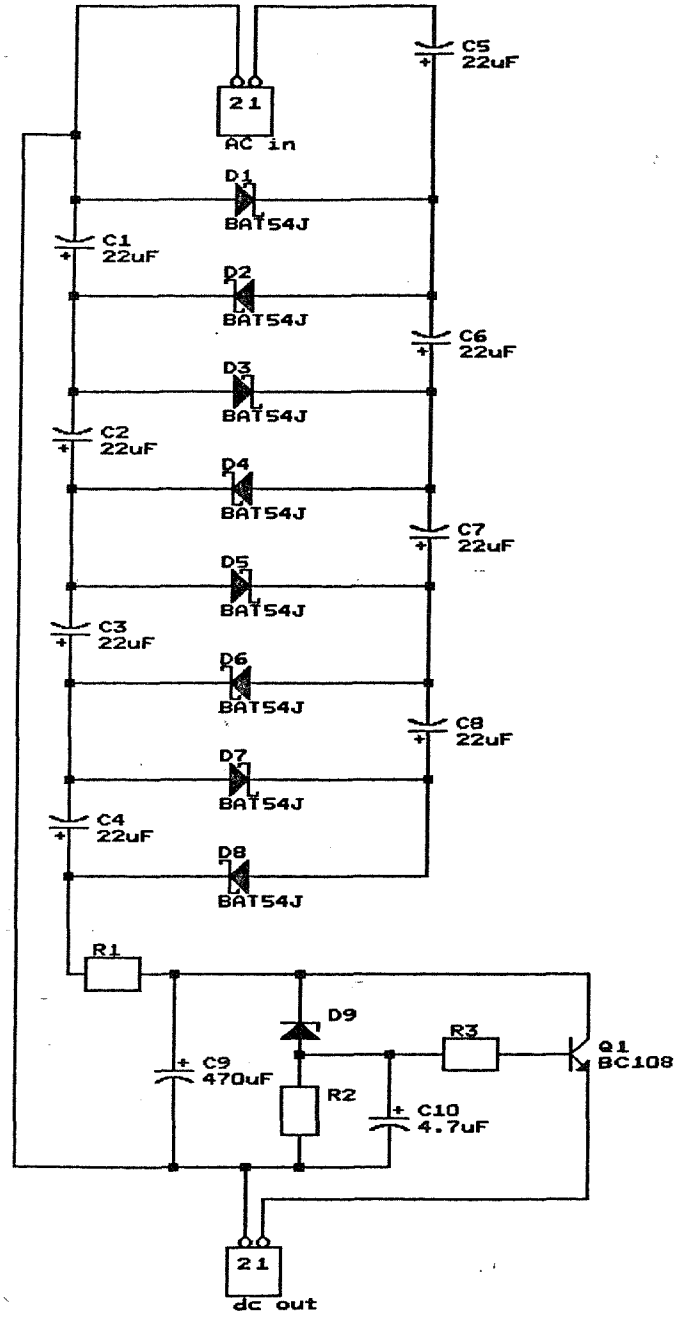

Figure 40: *Circuit diagram of the power management circuit*

6.2 Planar Based Power/Signal Transfer Theory

An external (planar) reader coil can be modelled as a circular loop antenna (in a resonant circuit), thus it is possible to calculate the magnetic field at a known location that is in close proximity to the coil (equation 6.14).

$$B = \frac{\mu_o I N a^2}{2\left(a^2 + r^2\right)^{3/2}} = \frac{\mu_o I N a^2}{2}\left(\frac{1}{r^3}\right) \quad if \quad r^2 >> a^2 \tag{6.14}$$

The magnetic field produced by the reader coil will induce a voltage into the planar SPMS coil. This induced voltage (that opposes the reader coil magnetic flux) can be modelled as shown in equation 6.15.

$$V = -N\frac{d\psi}{dt} \tag{6.15}$$

The magnetic flux through each turn can be defined as shown in equation 6.16.

$$\psi = \int B \cdot dS \tag{6.16}$$

The induced voltage (see equation 6.15) can be modelled further (leading to an expression for mutual inductance) using equations 6.14 and 6.16.

$$V = -N_2\frac{d\psi_{21}}{dt} = -N_2\frac{d}{dt}\left(\int B \cdot dS\right) \tag{6.17}$$

$$= -N_2\frac{d}{dt}\left[\int \frac{\mu_o I_1 N_1 a^2}{2\left(a^2 + r^2\right)^{3/2}} \cdot dS\right] \tag{6.17.1}$$

$$= -\left[\frac{\mu_o N_1 N_2 a^2 (\pi b^2)}{2(a^2 + r^2)^{3/2}}\right]\frac{dI_1}{dt} \qquad (6.17.2)$$

$$= -M\ \frac{dI_1}{dt} \qquad (6.17.3)$$

$$M = \left[\frac{\mu_o \pi N_1 N_2 (ab)^2}{2(a^2 + r^2)^{3/2}}\right] \qquad (6.18)$$

Using equations 6.15 and 6.16 a generalized expression[41] for induced voltage (at resonance) can be determined.

$$V = 2\pi f NSQB_o \cos\alpha \qquad (6.19)$$

For the experimental work described in this thesis the value of α is zero, because the two planar coils are on the same parallel plane, thus the term cosα can be ignored. It should be noted that in real life applications this will not always be the case because the coil on the micro-system may be aligned to the receiver/decoder coil at a finite angle or even a dynamic angle.

Theory suggests that it is possible to transfer energy across a planar coil for use in a micro-system. The theory also implies that a high Q value is beneficial when trying to maximize the induced voltage. Since $Q = f_0 / BW$ and the values of f_0 and Q will be fixed for a given coil, using two different frequencies on the same coil (one frequency for power transfer and a different frequency for the return data transfer) would not be efficient, unless the two frequencies were both within the operational half power BW. Such a small variation between power frequency and data frequency (about 2.5% for the prototype described later) would give rise to filtering problems within the reader.

One approach to powering and extracting data from a SPMS that is in close proximity to the external reader is to use backscattering. With this method data can be transferred from the SPMS to the reader by using a single frequency. The SPMS coil would need to be shunted for a short period of time, thus causing a brief measurable voltage drop on the external reader coil.

An alternative approach is for the SPMS planar coil to act as the primary coil for a brief period after the reader coil stops being the primary coil. This implies that the SPMS will need to store energy as data transfer will take place when there is no power being transferred from the reader coil. The SPMS will also require an internal frequency generator (with the associated stability issues).

6.2.1 Calculating An Optimal Diameter for the sensor-system Tx Coil

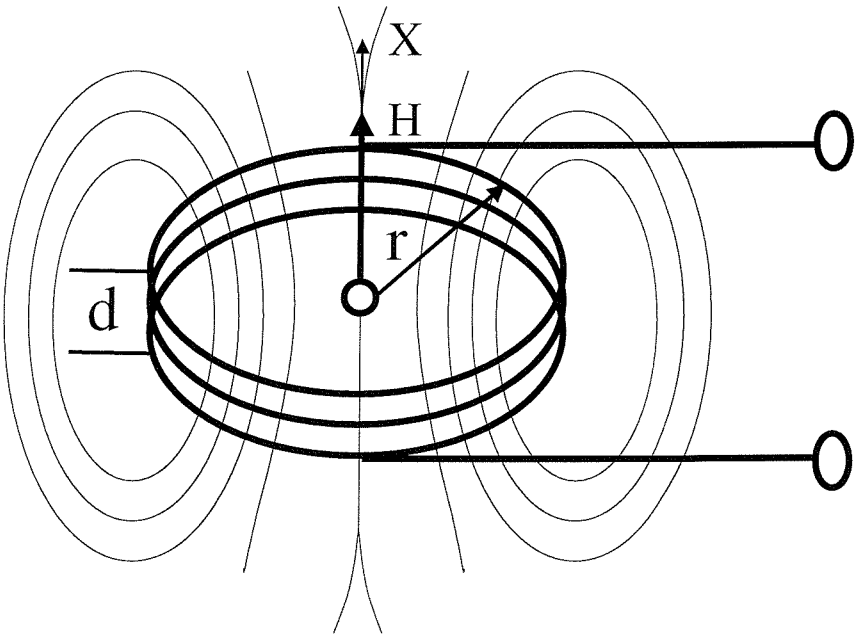

Figure 41: *The path of the lines of magnetic flux around a "short" cylindrical coil*

If the radius R (see figure 41) of the power Tx coil is varied at a constant distance x from the micro-system coil under the simplifying assumption of constant coil current I

in the Tx coil, then field strength H is found to be at its highest where $R \approx x$. This is not surprising because even where distance $x > 0$, an increase in radius R brings about a proportionate decrease in the field strength. A reduction in the radius R of the Tx coil where distance $x > 0$ brings about a reduction in the field strength $H(x) \sim x^{-3}$ in the case where the distance x is greater than the radius R. A change in the coil radius R at a constant distance x gives rise to the path of field strength H shown in figure 42. Field strength H increases rapidly where $x > R$; field strength H reaches a maximum where x=R, thereafter decreasing in proportion to the distance x.

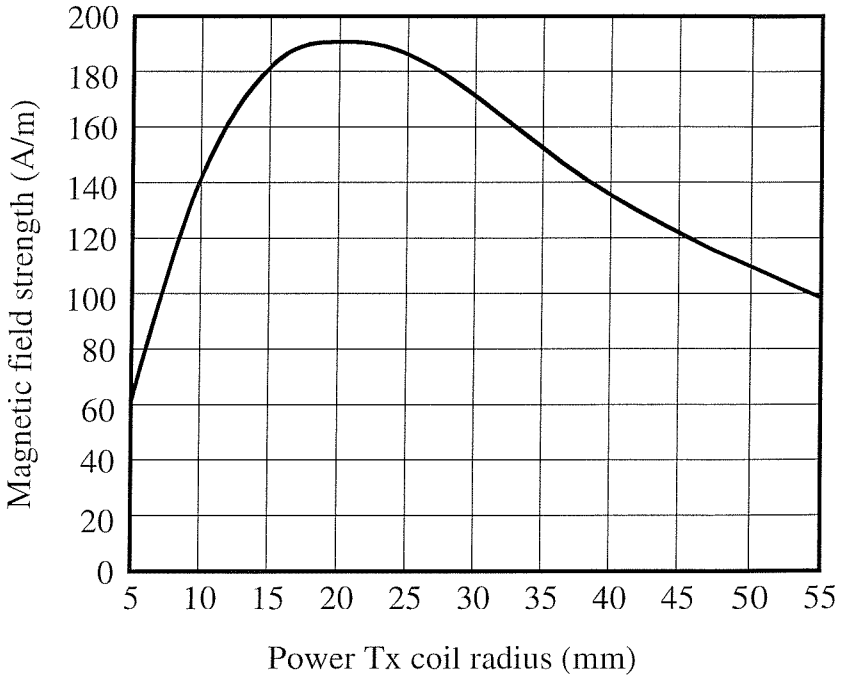

Figure 42: *The Variation in magnetic field strength H at a distance x=20mm*

The experimental work modeled here is important because it amounts to a feasibility study to determine if either of the above methods (or indeed a dual coil SPMS able to facilitate continuous power and data transfer) could be used for a SPMS in relation to sensor applications.

6.3 Planar Coil Experimental Setup

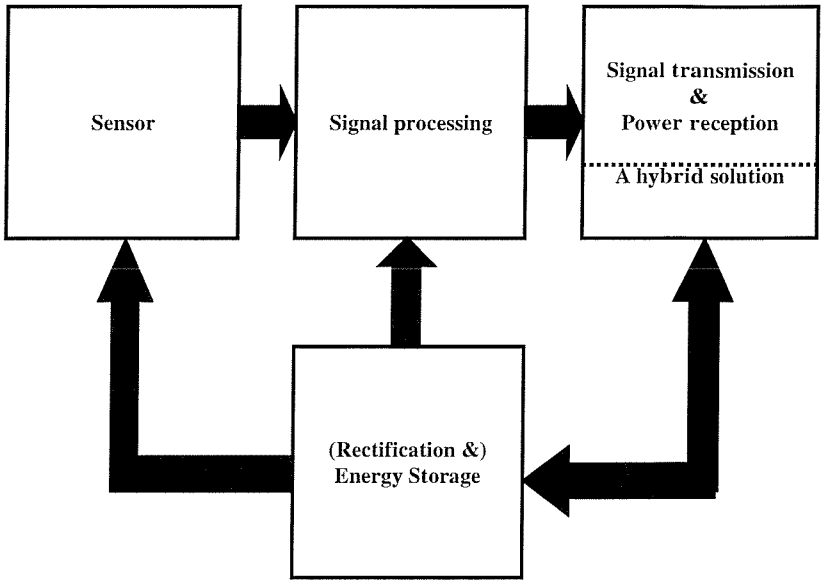

Figure 43: *Hybrid micro-system block diagram*

A test rig has been constructed as shown in figures 44 and 45. This consists of a pair of planar coils mounted in the same plane. Experiments have been conducted with coils of different sizes, different coil setups (see figure 45) and different values of inductance. A typical value of inductance may be 2.3μH. The resonant frequency of each coil (using a series capacitor of about 58pF) is 13.56MHz and the value of Q is about 40, provided the coil is driven via a series resistor of about 5Ω. The coil separation for maximum power measurements was set to 10mm. The wavelength associated with 13.56MHz is 22.12m, hence it is possible to exchange energy between the coils using a transformer-type (inductive) coupling. This is because the secondary coil can operate in the *near field* of the primary coil (i.e. the distance between the coils is significantly less than the crucial $\lambda/2\pi$ value where the near field ends).

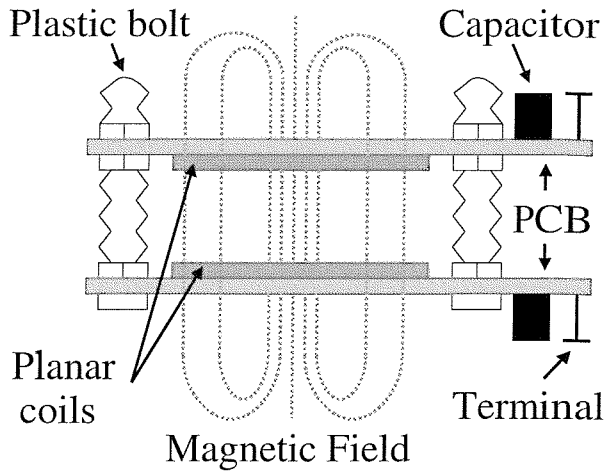

Figure 44: *Design of the planar coil test rig*

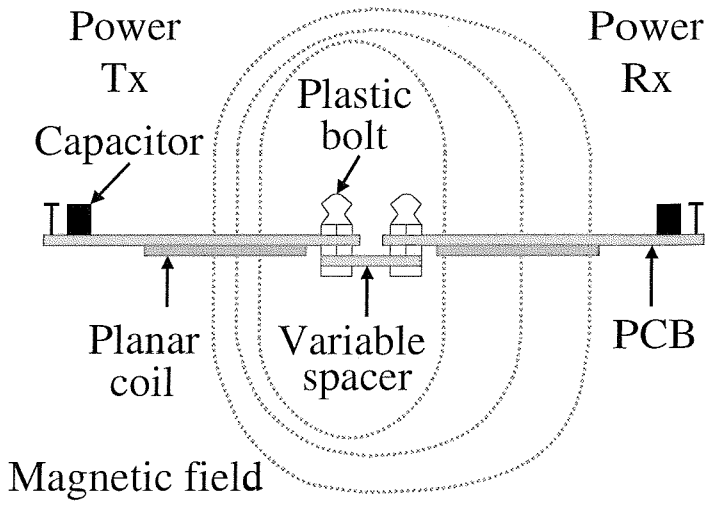

Figure 45: *An alternative test rig setup*

6.3.1 Results Of Initial Experimental Work

The resonant frequency of each planar coil was set to 13.56MHz by connecting an oscilloscope across the resonant circuit and tuning the capacitor value until a voltage peak was observed. By placing a resistive load on the output of the secondary coil rectifier it was possible to measure values of obtainable power. Values in excess of 15μW were observed for a 10mm coil spacing and a primary driving voltage of 8V (using the configuration shown in figure 44). Power available at the rectifier output was also measured for the frequencies located on the edge of the half power BW (13391kHz and 13730kHz). Values in excess of 4μW were observed. It was noted that power levels observed using the configuration in figure 45 were significantly

lower. This can be attributed partly due to the increased coil separation and lower flux density. Experimental problems are encountered as the SPMS coil moves further away from the reader coil, probably due to the rectifier input reducing in voltage to a value that is not sufficient for the rectifier to operate.

The results in figures 47 to 50 are for a primary coil driven via a 50Ω source at a voltage of 10V.

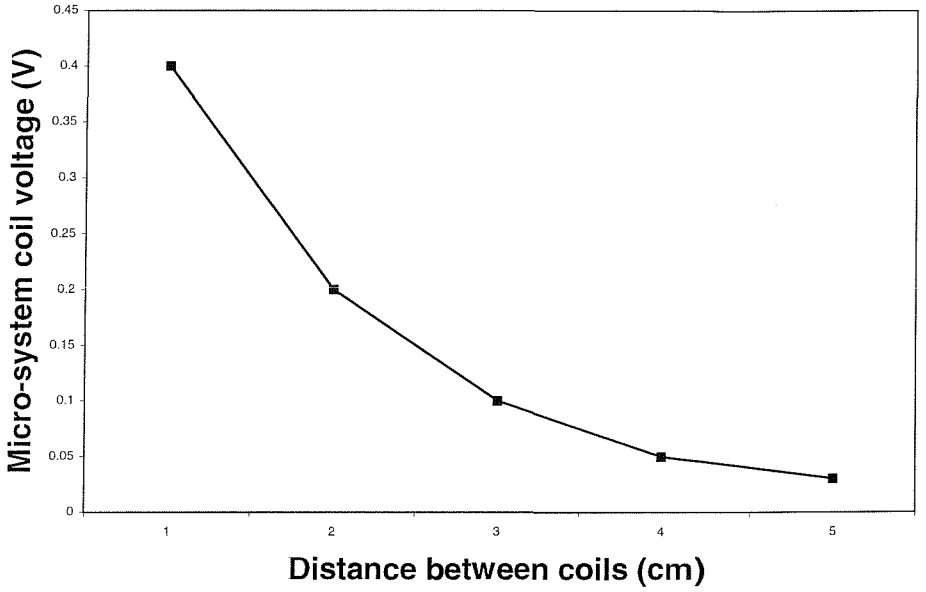

Figure 46: *Measured voltage using a 50Ω load*

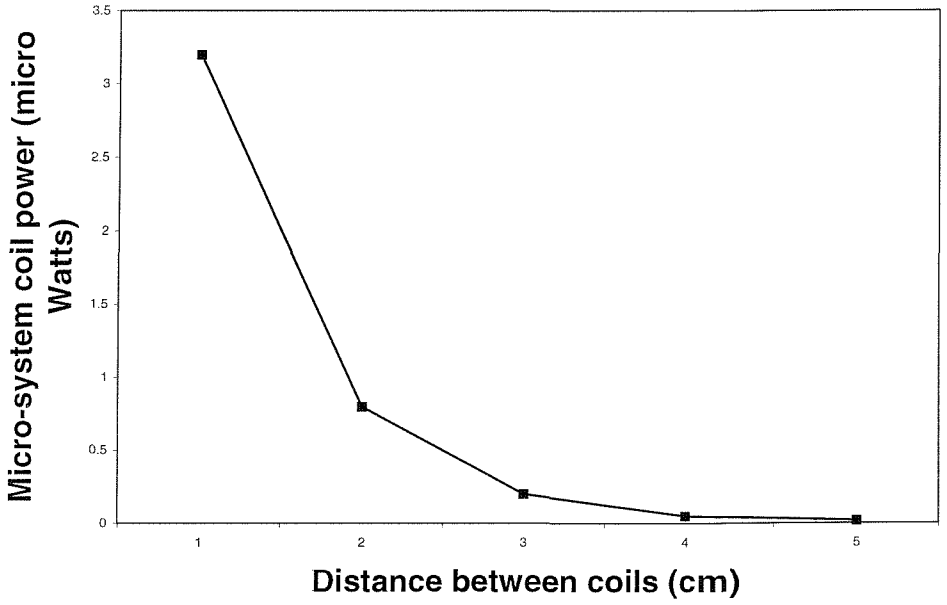

Figure 47: *Measured power using a 50Ω load*

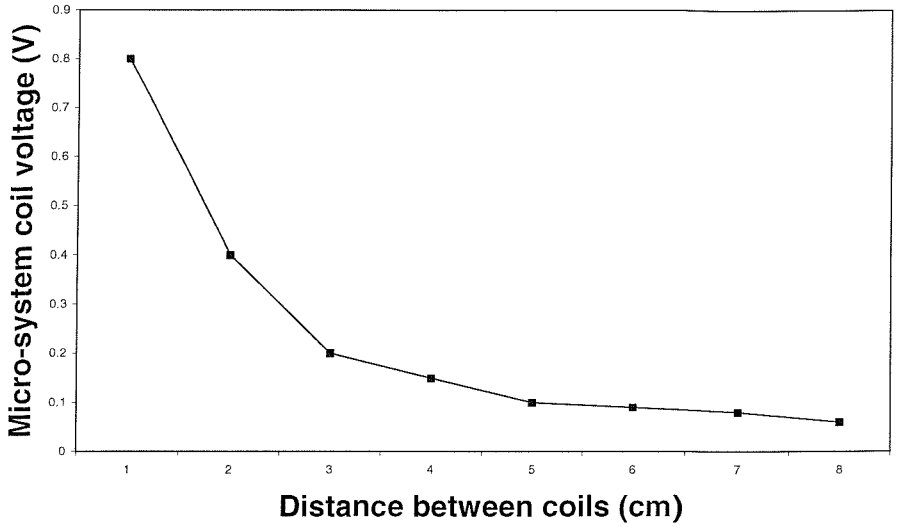

Figure 48: *Measured voltage using a 100Ω load*

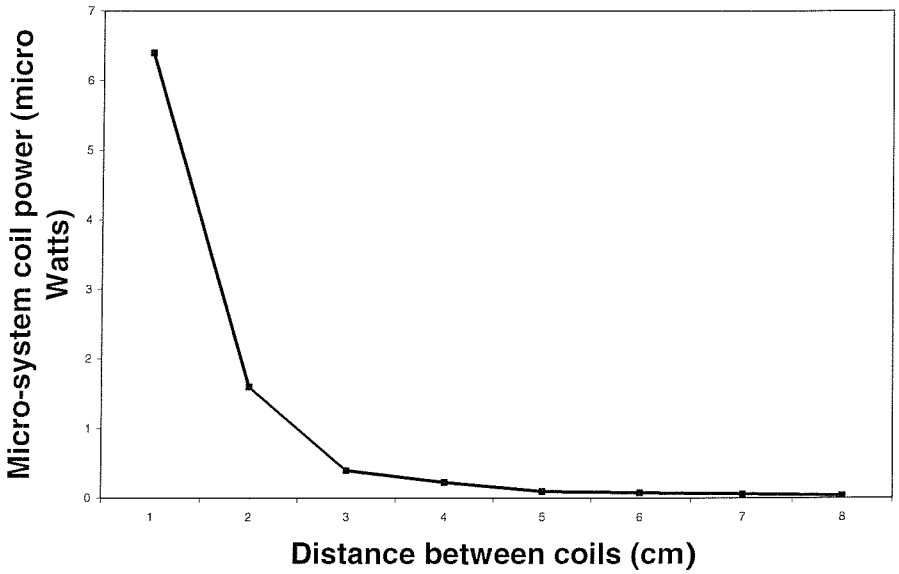

Figure 49: *Measured power using a 100Ω load*

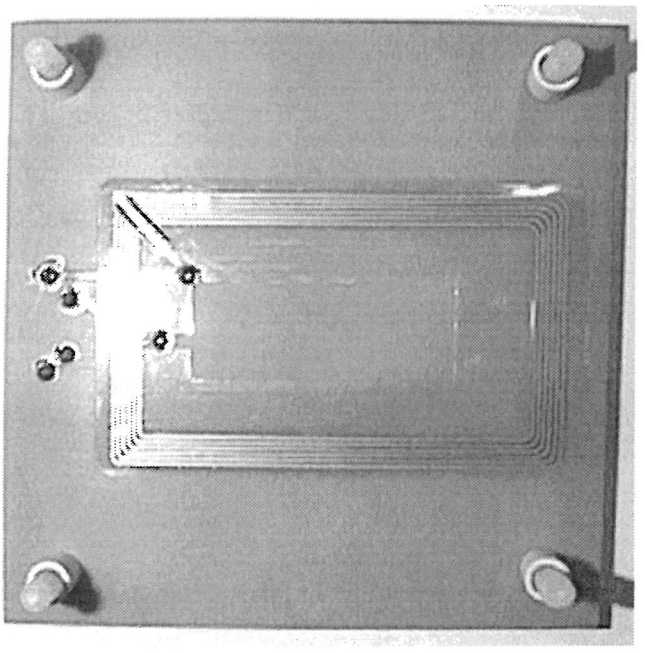

Figure 50: *A single planar test coil*

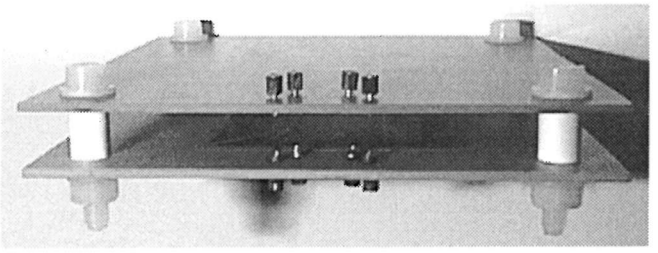

Figure 51: *Side view of the test rig*

6.3.2 Design Of The Receiver And Decoder

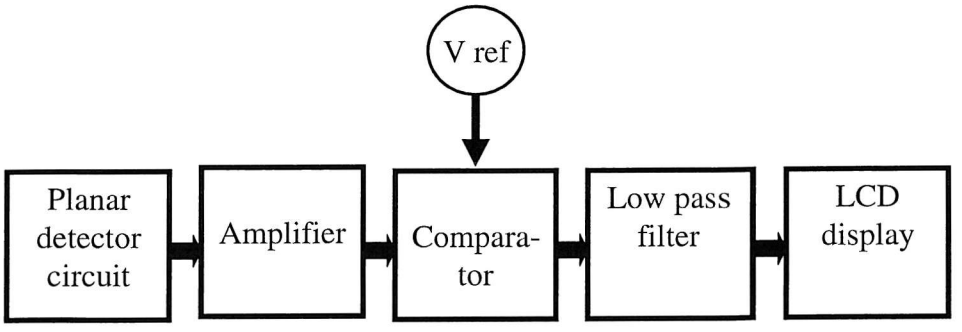

Figure 52: *Block diagram of the decoder*

Figure 52 shows a block diagram of the receiver and decoder circuit. The capacitor/coil combination has once again been tuned to operate at its resonant frequency. The receiver circuit is able to re-construct the PWM signal by comparing the amplitude of the received signal with a voltage reference. This approach is not ideal for all applications especially if the SPMS needs to operate in a noisy environment. For such operation further modulation would be required, however this would obviously increase the power requirements of the generator. Figure 53 shows a circuit diagram for the planar coil receiver. The design of this has been based on the design of the receiver used for the infra-red demonstrator in the previous chapter.

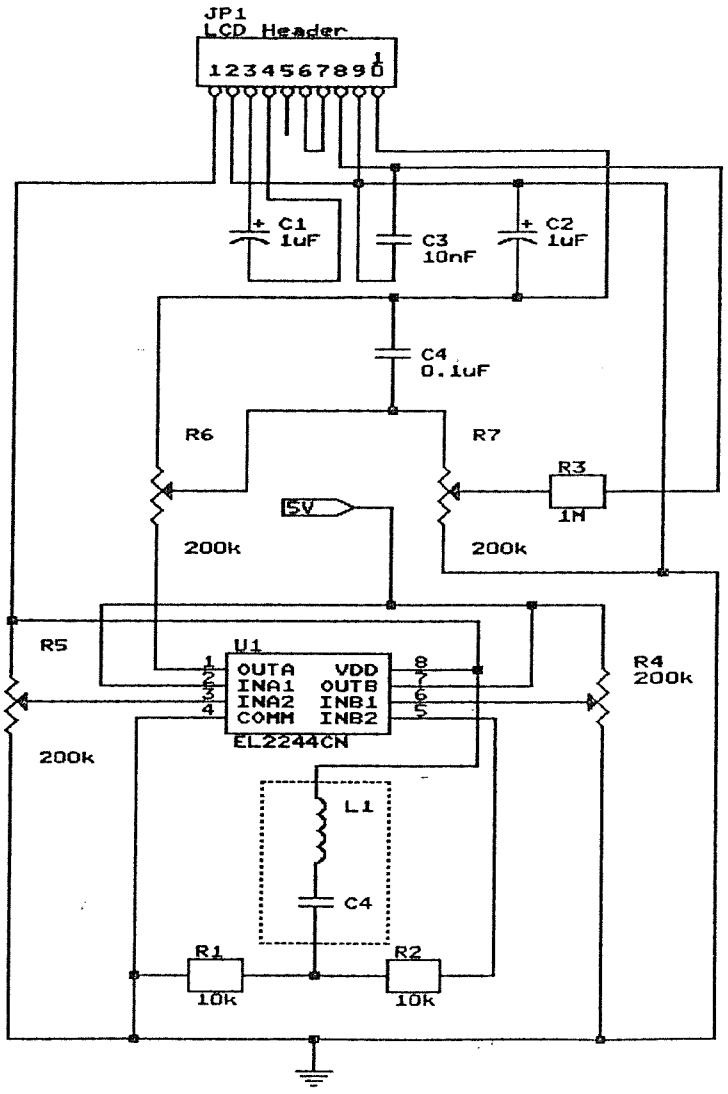

Figure 53: Circuit diagram of the planar based decoder

6.3.3 Calculation of the actual coil values

Both the transmitter coil and the receiver coil have been designed to operate at 1.2kHz.

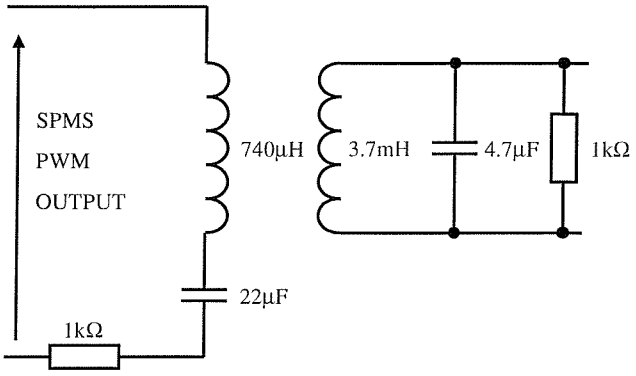

Figure 54: *The actual coil configuration used*

$f_{res} = 1 / (2\pi \sqrt{LC}) = 1.2$ kHz

$B = 1 / (2\pi RC) = 33$Hz

$Q = f_o / B = R (\sqrt{C/L}) = 35$

Coil dimensions:

SPMS coil = 30mm x 30mm x 5 turns (each 2mm wide)
Receiver coil = 60mm x 40mm x 5 turns (each 2mm wide)

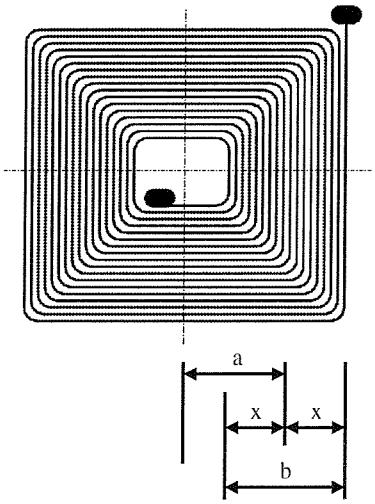

Figure 55: *Parameters for coil inductance calculation*

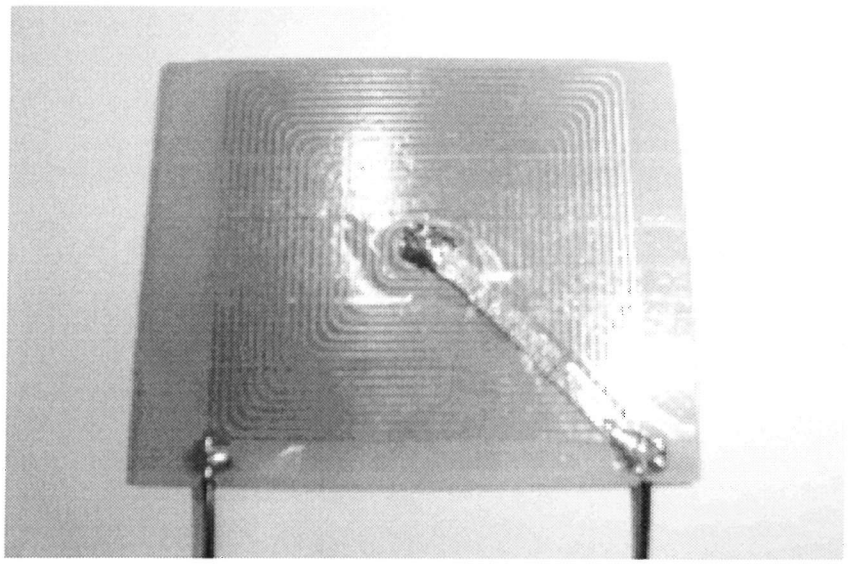

Figure 56: *The final coil design*

6.3.4 Optimisation Of The Required Power

There are numerous ways to reduce the overall power required by the SPMS. These include careful choice of circuit technology (for example using low power CMOS devices) and the communication algorithm. Using CMOS technology it is possible to design circuits which have virtually zero current demand between active cycles[42]. Enabling communication methods (like PWM) can also help to significantly reduce the amount of average power required by the communication circuit. Power conditioning systems (as illustrated in figure 58, by Kymissis et al[43]) may facilitate basic operation with very low power, however there is an overall reduction in the amount of data received from the sensor and there is a need to include (hence power) a trigger circuit to activate communication. Given the relationship between magnetic field with distance for near field operation (see figure 57) any potential power savings may ultimately be used to facilitate communication over greater distances.

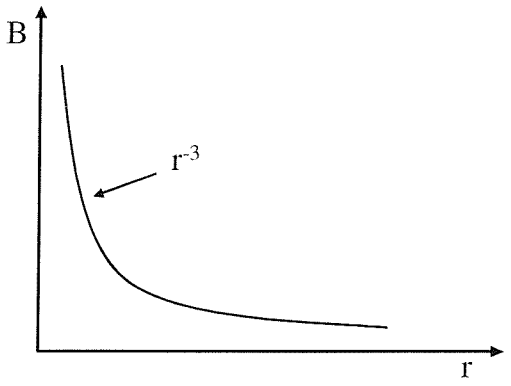

Figure 57: *Decaying of magnetic field with distance*

Equation 3.14 indicates that the magnetic field strength decays with $1/r^3$. A graphical representation is shown in figure 57. It has a maximum amplitude in the plane of the loop and is directly proportional to both the current and the number of turns.

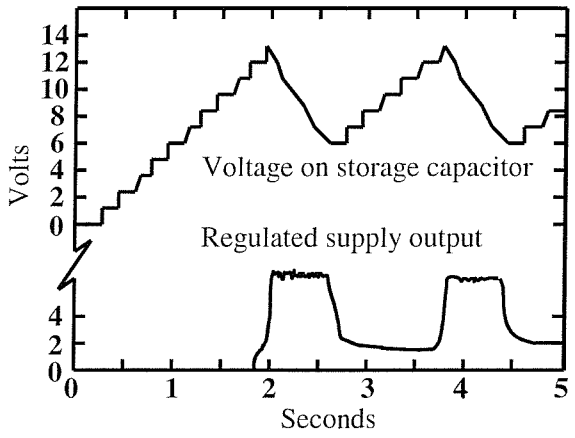

Figure 58: *Example operation of a power conditioning system*[43]

The top trace in figure 58 shows how a capacitor within a SPMS can be used to store an increasing amount of charge until it is time for communication to take place (as shown by the lower trace). This figure outlines a general principle that can be applied when there is not enough energy available for continuous communication. It can be seen that there is not enough energy available in this example by virtue of the top trace taking a downward trend during communication.

6.3.5 Signal Extraction Using Backscattering

For some applications it makes sense to use the planar coil not just for transferring energy into the micro-system, but to also extract the data from the micro-system. Backscattering refers to the process of shunting (i.e. loading) the micro-system coil such that a voltage drop can be observed across the external coil. Because the micro-system coil is in the near field of the external coil, the process of backscattering can be modeled by using a conventional transformer with a referred load (see figure 59).

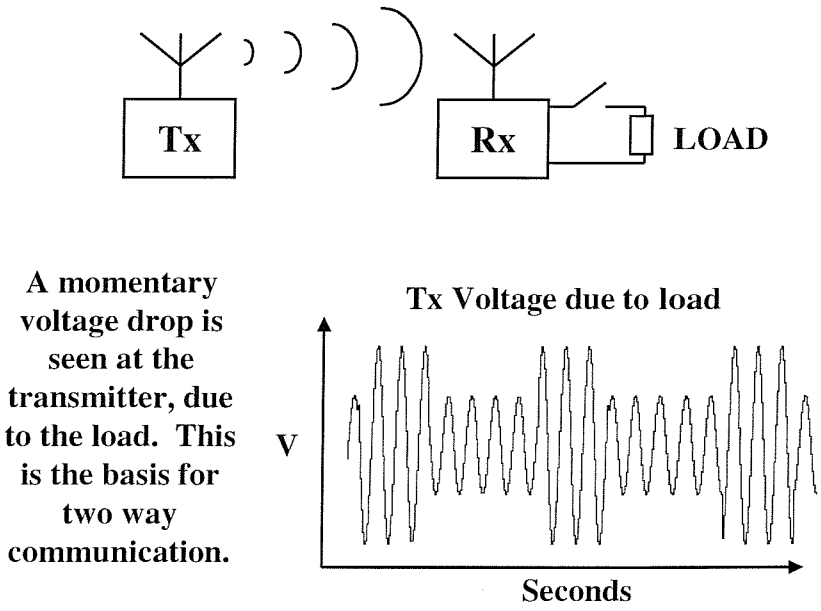

Figure 59: *Backscattering as a communication method*

6.4 Conclusions

Experimental results have shown that with careful consideration of design parameters it is possible to design a SPMS employing planar energy transfer for data communication. Such a system is well suited to sensor applications. Some of the key design parameters have been identified. Experiments were conducted on coils that measured about 85mm x 55mm, however further work could potentially reduce the overall coil size and implement power efficient communication algorithms. It is anticipated that current SPMS research relating to the general concept of a self-powered wireless sensor system is an area due to expand significantly in the near future.

Chapter 7

7. Development of a Radio Micro-System Demonstrator

7.1 Introduction

This chapter details the development of a SPMS that has been designed to communicate via a radio link. Using a radio frequency to communicate has many advantages over the systems described in chapters 4 and 5. As with the planar system described in chapter 6, a radio system can be fully encapsulated or embedded. This in itself opens up a wide range of potential applications, especially those associated with dirty environments or locations where the sensor-system can not be in direct line of sight with the receiver/decoder or, in the case of the LCD, the operator. Radio technology is also compatible with standard substrate based fabrication technology. It would certainly be feasible for both the sensor electronics and radio transmitter to be integrated on the same substrate using these techniques. This approach has further benefits of reducing the micro-system size and, potentially, overall production costs.

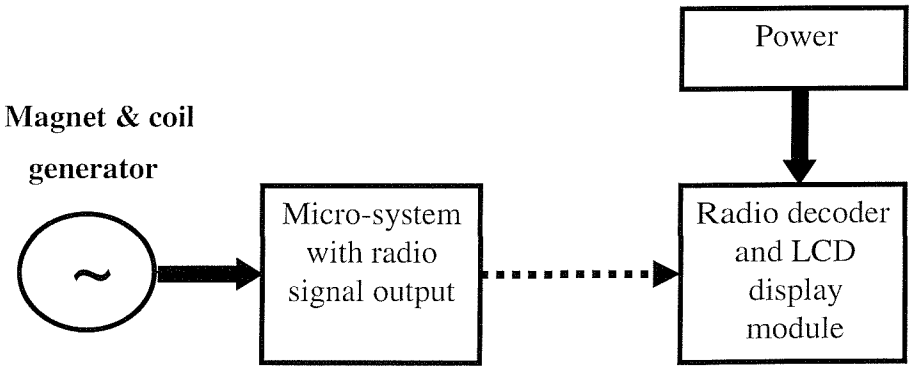

Figure 60: *Block diagram of the SPMS and its associated radio decoder*

Figure 60 shows a block diagram of the radio based sensor system and its associated receiver/decoder. The magnet-coil generator is the same generator that was used in the previous optical based micro-system. This generator is once again used to power a sensor system comprising of power management circuitry, sensor and a radio transmitter. Figure 61 also shows the decoder and display module. As with the IR receiver, this can have its own external power supply as it is remote from the sensor-

system. As in the previous three chapters, the function of the decoder is to re-construct the data radiated by the sensor-system and display it on a LCD.

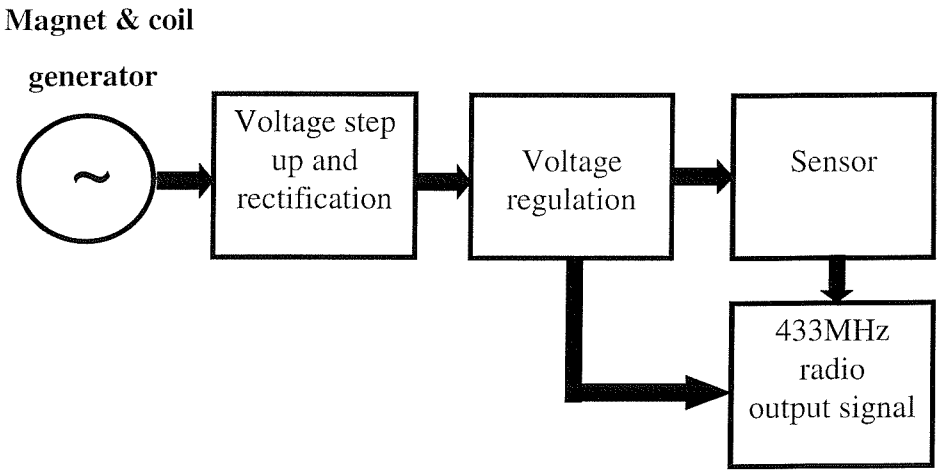

Figure 61: *Block diagram of the SPMS*

Figure 62 shows a circuit diagram for the SPMS. The basic circuit is similar to the circuit described in chapter 6 to communicate via planar coil, only this system is utilizing a 433MHz radio module. As outlined in chapter 2, the 433MHz band is a legal frequency for such a system to use in the UK. As such a number of commercial transmitter modules exist. With such modules there is always a trade off between power consumption and transmission distance. For this specific system it was deemed that a low power solution was more important than transmission distance and this formed the basis of a search for a suitable transmitter module. The module used is a low power and low cost am transmitter/receiver pair sold by Maplin electronics. An fm module would have been the first choice for this system, as such modules are less prone to noise that would be re-produced by the decoder and such modules also tend to use equal amounts of power or maybe even less power then an am module given the less complex transmitter design. The final choice of module was partly decided by cost, as the low power modules tend to be cheaper then comparable fm modules.

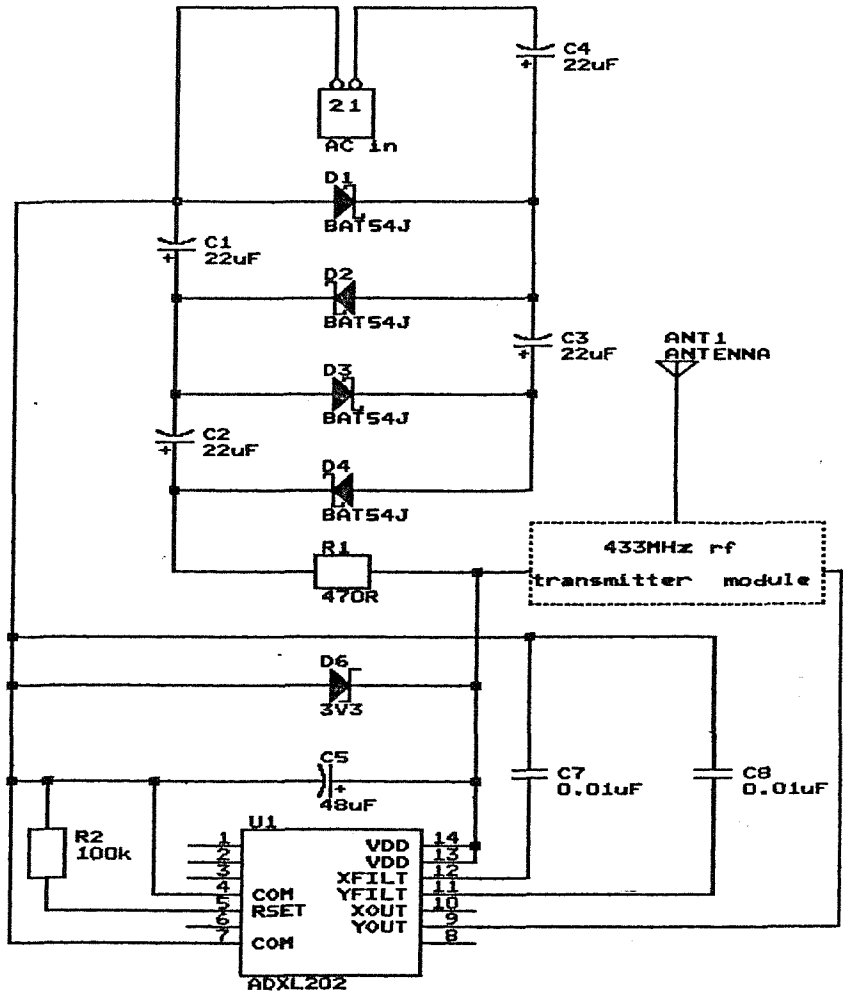

Figure 62: *Circuit diagram of the radio based micro-system*

It can be seen in figure 62 that the sensor and the radio transmitter share a common power supply. Given that the power used by the am transmitter is dependent in part on the output signal from the sensor it was thought that the sensor may benefit from its own voltage step-up circuit.

Spice simulations were carried out to see how the transmitter module affected the supply voltage to the sensor and the manufactures data sheet for the sensor was consulted to find out how this related to variations in sensor accuracy. The spice simulation in figure 63 shows that the supply voltage (with the transmitter module powered up, but not transmitting) was within the operational supply voltage as required by the sensor. With the transmitter module powered up, but not transmitting the simulated system voltage was 3.8V. With the transmitter powered up and transmitting, the simulated system voltage fell to 3.5V. This is still within the

operational limits for the sensor, however a change in input voltage will affect accuracy. In this case the accuracy of the sensor would be affected by 4%. It was decided that 4% error was not significant enough to warrant having two separate step up circuits. The benefit of not having two step up circuits is also seen in the overall SPMS size.

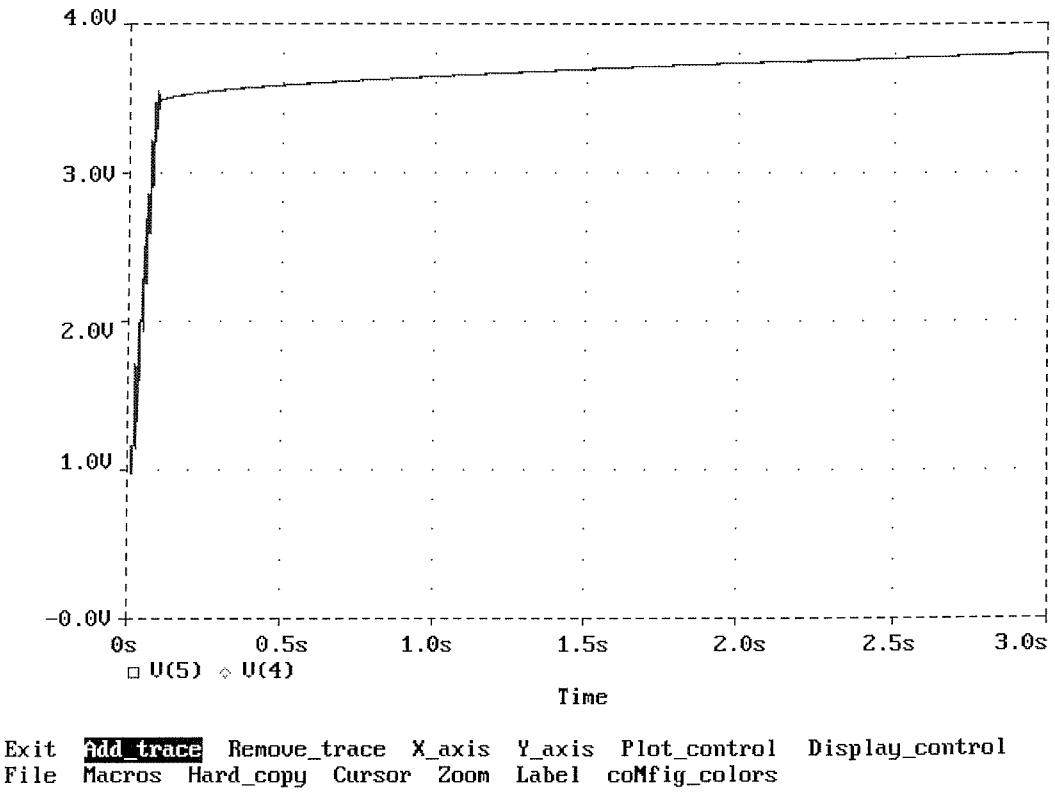

Figure 63: *Spice simulation of the voltage step up circuit with radio tx*

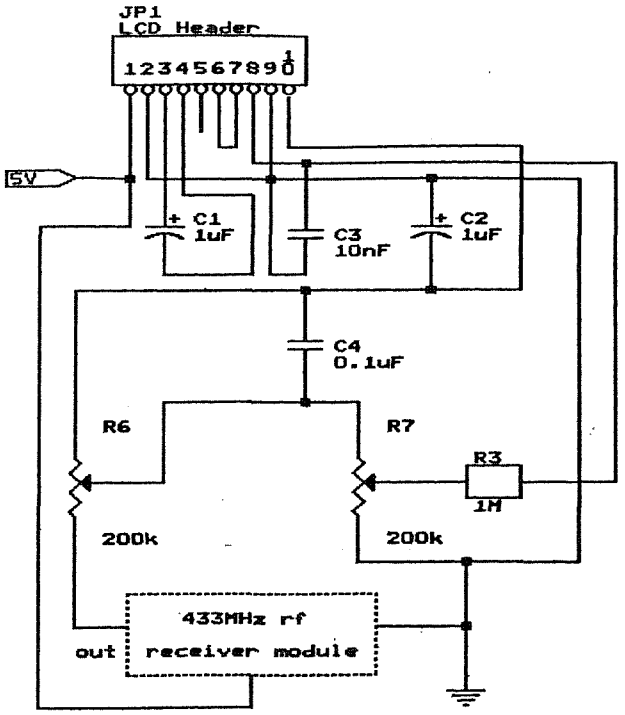

Figure 64: *Circuit diagram of the radio based micro-system receiver*

Figure 64 shows a circuit diagram of the radio based micro-system receiver. The 433MHz receiver module only requires a power supply from the system to operate and its output signal that is still in a PWM format is converted into an average dc voltage and this voltage is then fed into the analogue to digital converter that is built into the LCD module. R6 and R7 can be used to control the system calibration and sensitivity. As with the previous demonstrators a sensitivity of 2mg has been achieved.

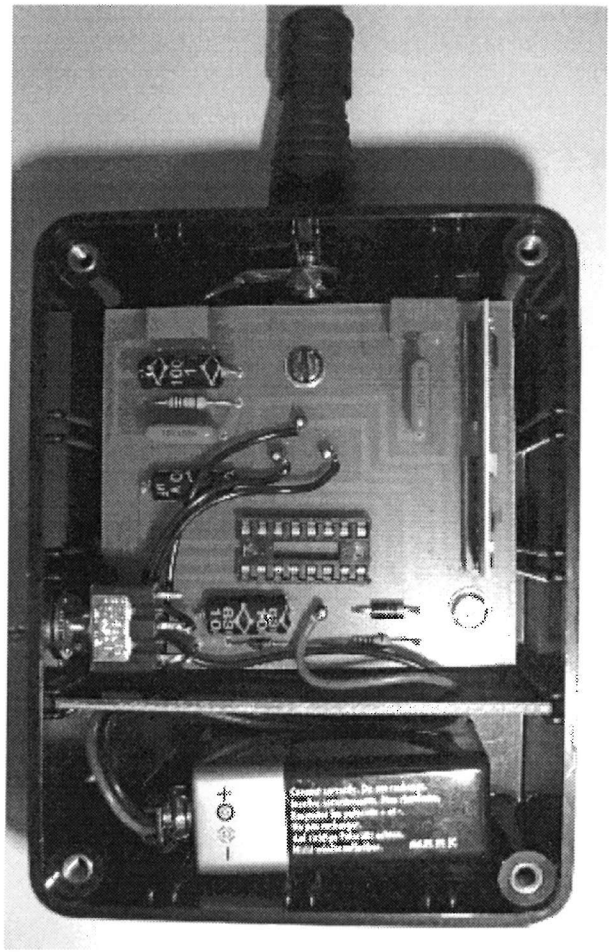

Figure 65: *Picture of the radio SPMS (with front cover removed)*

Figure 65 shows the physical PCB layout of the final radio receiver system. A battery has been used to make the system portable. The receiver has not been optimized for size given that this is not likely to be of commercial interest and the main focus for efficient use of space has been the actual SPMS with its associated transmitter module. Four aerial designs have been tested on the final prototype and figure 66 shows the maximum distance achieved with each design. Loop 1 was a wire of 30cm in length and loop 2 was a wire of 5cm in length. The loop aerials were very directional as expected, but the best all round aerial tested was arguably the whip aerial.

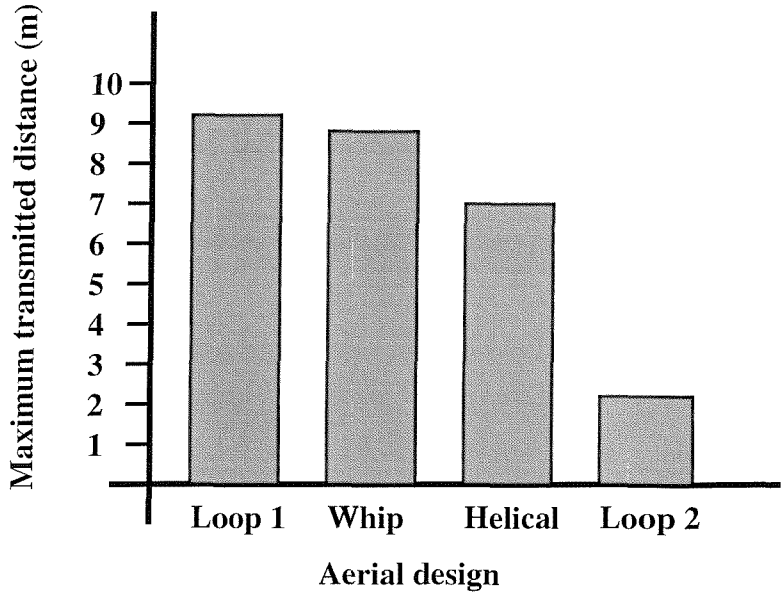

Figure 66: *Measured operational distance with different aerial types*

Table 10 shows the fundamental advantages and disadvantages for each aerial design that was tried on the demonstrator system.

Advantages / disadvantages of each antenna design			
Feature	Helical	Loop	Whip
Performance	ok	poor	good
Ease of Design	ok	poor	good
Size	good	ok	poor
Immunity to hand detuning and or components in close proximity	ok	good	poor

Table 10: *Properties of three different aerial designs*

7.2 Conclusions for the radio based demonstrator

The radio based demonstrator combines knowledge gained through the development of the LCD, infra-red and planar based demonstrators and it adds the flexibility that a radio solution can offer in terms of communication distance (metres, not centimetres) and ease of operation even when the SPMS and receiver are not in the line of sight. The system developed has been shown to fully function with continuous operation

over many hours (without failure) when powered by the micro-generator described in chapter 3. The limits of operation for this system have not been fully tested and this would form the basis for interesting future research.

Chapter 8

8. Conclusions

An electromechanical power generator whose operating principle is based on the relative movement of a permanent magnet with respect to a coil has been designed and fabricated. The feasibility studies and experimental results have demonstrated the potential of such a device for self-powered systems. The prototype occupies a maximum space of 240mm^3 including the space required for the maximum deflection. Within this space, generation of useful electrical power of 0.53mw has been practically achieved. This power corresponds to 25μm amplitude of vibration at an excitation frequency of 322Hz. The results have clearly shown that generation of practical amount of power within a small space is now possible and that the elimination of batteries for certain applications with modest frequencies is also feasible.

In its present form the LCD based demonstrator that has been developed is fully functional, however there are a number of improvements that can be made to address a range of issues like size, power consumption, mode of communication, reliability and weight.

The minimum force required for the SPMS to operate could be reduced by using a power control circuit. This could be a Programmable Interrupt Controller (PIC) that has two key functions. To provide a soft start for the circuit, thus preventing a turn on power surge and to turn blocks of the circuit on and off as required. For the specific demonstrator described in this chapter, a PIC could be used to power manage the accelerometer and the LCD display. For future demonstrators it would also be possible to use a PIC to pre-process data or control communication.

One significant limitation of this demonstrator is the need to view a display that is based on the SPMS. For most real life applications it would be better to have a different method of communication. Infra-red and radio solutions are just two approaches that would potentially create a more versatile system.

In its present form the infra-red based SPMS is fully functional and a significant improvement in size has been realised when compared to the LCD based demonstrator. Another significant improvement is with the overall weight of the

system. This has been reduced, as a transformer is no longer required. The demonstrator could be improved by using a different communication protocol. PWM is not ideal both in terms of power efficiency and reliability. The diode-capacitor step up circuit has proved to be very reliable and a significant advance on the use of a transformer.

Experimental results have shown that with careful consideration of design parameters it is possible to design a SPMS employing planar energy transfer for both power and data. Such a system is well suited to sensor applications. Some of the key design parameters have been identified. Experiments were conducted on coils that measured about 85mm x 55mm, however further work could potentially reduce the overall coil size and implement power efficient communication algorithms. It is anticipated that current SPMS research relating to the general concept of a self-powered wireless sensor system is an area due to expand significantly in the near future.

Chapter 9

9. Future Work

Due to the wide scope of this thesis there are indeed many areas that could form the basis for future work, most of which would be novel. This section is intended to give a feel for the range of areas that could follow on directly from the work that has been documented in this thesis.

9.1 Optimisation

9.1.1 The vibration based generator

The vibration based generator could be optimised in numerous way. The existing material used for the generators beam has exhibited stress at high amplitudes of vibration and it would therefore be worth investigating alternative materials that may be suitable. Both the size and weight of the generator could be significantly reduced without much re-design, as the device is over engineered at present. An increase in the number of coil turns could be used to increase the generated voltage and therefore reduce the size of the step up circuit. Such a change may also increase the efficiency of the system. The generator could have vibration stops added, thus enabling it to operate in areas where there is a very diverse range of vibration amplitudes, such that mechanical damage could occur. The choice of resonant frequency could be increased and in theory this would also increase the amount of power generated. The magnets could be screen printed and the coil could even be micro-machined.

9.1.2 The overall micro-system

A hybrid design approach could be used to reduce the overall size of the SPMS and application specific devices could be created. Given a specific application the potential for optimization would be greatly increased.

9.2 PIC Control

The use of a PIC would make it easy to use efficient protocols for data transfer and the addition of 'intelligence' could also be used to pre-process data, thus deducing the amount of power required for communication. A PIC would also introduce more functionality and adaptability. This could lead towards the design of a generic system that could be programmed for a given application. Such an approach would have huge commercial implications.

9.3 Micro-system networks

Generic design could be used to create micro-systems able to communicate with each other in a distributed system. Issues relating to data communication may also need to be re-addressed for such an approach to be viable. Such distributed micro-systems could have commercial potential for applications where numerous sensors are required in an in-accessible location. Potential applications could be probe related, in space for example.

9.4 Energy storage

The development of a micro-system that is able to store power would facilitate communication over greater distances than would be feasible with a micro-system that operates continuously. A novel area of research is the control of such power, as there are many different approaches to decide when to use such power. The storage media is also an area that could be addressed, especially for low vibration environments where the amount of power being generated is potentially similar to the amount of power being lost through leakage of the storage mechanism. To determine if power storage is indeed required, a study into the limits of conventional (continuous) operation could be carried out. It is however clear that for applications where communication over a large distance is a requirement, power storage could enable communication to be viable thus filling a potential market niche.

9.5 Applications

The work detailed in this thesis has significant commercial potential. Future work could focus on the integration of existing technology into real life environments. Typical real life environments include military, domestic, industrial, environmental and space to name but a few.

References

[1] S Jacobs. *Battery Technology choices for RF-ID Tags.* Tadiran Electronic Industries Inc., Port Washington, New York. http://rapidttp.com/transponder/tadiran.html

[2] P Glynne-Jones, M El-hami, SP Beeby, EP James, AD Brown, M Hill, NM White. *A vibration-power generator for wireless Micro-systems.* International Symposium on Smart Structures and Micro-systems (IS3M 2000), 2000.

[3] T Starner. *Human powered wearable computing.* IBM Syst. *J.*, Vol. 35, Nos. 3-4, 1996, pp. 618-629.

[4] DM Rowe, DV Morgan and JH Kiely. *Low cost miniature thermoelectric generator.* Electron. Lett., 27, 1991, pp. 2332-2334.

[5] M Hayakawa. *Electronic wristwatch with generator.* US patent 5001685, 1991.

[6] D Friedman, H Heinreich and DW Duan. *A low-power CMOS integrated circuit for field-powered radio frequency identification tags.* ISSCC Dig. Tech. Papers, Feb. 1997, pp. 294-295.

[7] J Bouvier, Y Thorigne, SA Hassan, MJ Revillet, P Senn. *A smart Card CMOS circuit with Magnetic Power and Communications Interface.* International Solid State Circuits Conference, 1997, pp.206-207.

[8] LA Geddes. *Historical highlights in cardiac pacing.* IEEE Eng. Med. Biol, June 1990, pp. 12-18.

[9] *Self-powered Micro-systems (SPMS).* USITT Univ. of Southampton. http://www.usitt.ecs.soton.ac.uk/selfpower.shtml

[10] N Scholey. *Rechargeable batteries for mobile communication.* Electronics & Communication Engineering Journal, vol. 7, No. 3, June 1995, pp.93-96.

[11] R Amirtharajah, AP Chandrakasan. *Self-powered signal processing using vibration-based power generation.* IEEE Journal of Solid State Circuits, vol.33, No.5, 1998, pp.687-695.

[12] M El-hami, P Glynne-Jones, E James, S Beeby, NM White, AD Brown, JN Ross, M Hill. *A new approach towards the design of a vibration-based micro-electromechanical generator.* Accepted for publication, Euro-sensors 2000.

[13] CB Williams, RB Yates. *Analysis of a micro-electric generator for micro-systems.* Journal of Sensors and Actuators, vol.52, No.1-3, 1996, pp.8-11.

[14] Korea Institute of Science and Technology (KIST) press release. http://www.dynamixcosmo.com/battery.html

[15] Case for support: Self-powered micro-systems. University of Southampton, Dept. of Electronics & Computer Science, Research proposal.

[16] JN Ross. *Optical power for sensor interfaces.* Journal of Measurement Science & Technology, vol.3, No.7, 1992, pp.651-655.

[17] TB Cho, DW Cline, CSG Conroy, PR Gray. *Design Considerations for High-Speed Low-Power Low-Voltage CMOS Analogue-to-Digital Converters.* University of California at Berkeley. http://kabuki.eecs.berkeley.edu/~tcho/

[18] M Marsh. *Transponder News, Designing RF-ID systems.* March 2000. http://rapidttp.com/transponder/taglayer.html

[19] D Friedman, H Heinrich, D Duan. *A low-Power CMOS Integrated Circuit for*

Field-Powered Radio Frequency Identification Tags. IEEE International Solid State Circuits Conference, 1997, pp.204-205.

[20] B Warneke, C Chang. *Ultra-Low Power Communication Logic Circuits for Distributed Sensor Networks.* 1998 EECS 241 UC Berkeley. http://www-bsac.eecs.berkeley.edu/~bwarneke/ee241/

[21] Research by Oak Ridge National Laboratory. *"Wireless Sensors – Buyer Beware".* http://www.sensorsmag.com/articles/0401/18/main.shtml

[22] Stordeur, Matthias, Stark, Ingo. *Low power Thermoelectric Generators – innovative self-sufficient energy sources for sensor and micro systems.* International Association of Sensorics. Sensors, Transducers and Systems conference, 1999, proc.2, pp.193-198.

[23] British Standards Institute. BS 5501:Part 1:1977 EN 50014, *Electrical apparatus for potentially explosive atmospheres, General requirements,* pp.5.

[24] Transponder News. *Standards relating to Transponders.* http://rapidttp.com/transponder/standard.html

[25] Transponder news. *Radio frequency issues relating to Transponders.* http://rapidttp.com/transponder/frequenc.html

[26] K Finkenzeller. *RF-ID Handbook.* ISBN 0-471-98851-0, pp.111-124 and 275-284.

[27] Data monitoring by low power radio. http://www.pacs.co.uk/

[28] S Woodward. *Light powers isolation amplifier.* University of North Carolina. http://www.ednmag.com/reg/1999/012199/02di.htm#light

[29] W Kuntz, R Mores. *Electrically Insulated Smart Sensors: Principles for Operation and Supply.* Journal of Sensors and Actuators, vol.26, No.1-3, 1991, pp.497-505.

[30] AM Niknejad. *Analysis, design, and optimisation of spiral inductors and transistors for SI RF ICs.* University of California, Berkeley. http://formosa.eecs.berkeley.edu/~niknejad/

[31] H Matsuki, M Yamaguchi, T Watanabe, K Murakami. *Implantable transformer for an artificial heart utilizing amorphous magnetic fibres.* Journal of Applied Physics, 1998, pp.5859-5861.

[32] B Warneke, C Chang. *Ultra-low power communication logic circuits for distributed sensor networks.* 1998 UC Berkeley. http://www-bsac.eecs.berkeley.edu/~bwarneke/ee241/midterm.html

[33] NM White, GR Leach. *Fabrication of a thick film sensor employing an ultrasonic oscillator.* IEE Proc.- Science Measurement and Technology, vol.142, No.3, 1995, pp.249-254.

[34] MC Smayling. *VLSI CMOS technology for low power sensor applications.* Journal of Solid State Ionics, vol.34, No.1-2, 1989, pp.121-125.

[35] EA Vittoz . *Low-Power Design: Ways to Approach the limits.* IEEE International Solid State Circuit Conference, 1994, pp.14-15.

[36] MR Al-Mohanadi, JN Ross, JE Brignell. *Optical power and intelligent sensors.* Journal of Sensors and Actuators, vol. 60, No.1-3, 1997, pp.142-146.

[37] Forrest M Mims III. *Getting started in electronics*, Radio Shack (a division of Tandy) book, catalogue number 276-5003.

[38] WT Thompson. *Theory of vibration with applications*. Prentice-Hall, Englewood cliffs, 1972.

[39] Opera 2d and 3d, "Reference and user guide". Vector Fields Ltd., Oxford.

[40] C. Jackson. *The Practical vibration primer*. Houston: Gulf Pub. Co., 1979 pp. 44 fig 8-2

[41] Microchip™ Technology Inc. *125kHz RF-ID System Design Guide*. 1998 http://www.microchip.com/10/Lit/RFID/Guides/51115e/index.htm

[42] MC Smayling. *VLSI CMOS technology for low power sensor applications.* Journal of Solid State Ionics, vol.34, No.1-2, 1989, pp.121-125.

[43] J Kymissis, C Kendall, J Paradiso, N Gershenfeld. *Parasitic Power Harvesting in Shoes.* MIT Physics and Media Group, 1998. Contact: johnkym@media.mit.edu.